JÉSSICA RIBEIRO SOARES

Age-dependent miR156-targeted *SPLs* are required for extrafloral nectary development and ecological relationships in *Passiflora* spp.

Thesis submitted to the Plant Physiology Graduate Program of the Universidade Federal de Viçosa in partial fulfillment of the requirements for the degree of *Doctor Scientiae*.

Adviser: Wagner Campos Otoni

VIÇOSA-MINAS GERAIS

2024

Ficha catalográfica elaborada pela Biblioteca Central da Universidade Federal de Viçosa - Campus Viçosa

T
S676a
2024

Soares, Jéssica Ribeiro, 1992-
Age-dependent miR156-targeted SPLs are required for extrafloral nectary development and ecological relationships in *Passiflora* spp / Jéssica Ribeiro Soares. – Viçosa, MG, 2024.
1 tese eletrônica (72 f.): il. (algumas color.).

Texto em inglês.
Orientador: Wagner Campos Otoni.
Tese (doutorado) - Universidade Federal de Viçosa, Departamento de Biologia Vegetal, 2024.
Inclui bibliografia.
DOI: https://doi.org/10.47328/ufvbbt.2024.524
Modo de acesso: World Wide Web.

1. Regulação de expressão gênica. 2. Passifloraceae. 3. Nectários. 4. Análise foliar. 5. Plantas - Desenvolvimento. I. Otoni, Wagner Campos, 1962-. II. Universidade Federal de Viçosa. Departamento de Biologia Vegetal. Programa de Pós-Graduação em Fisiologia Vegetal. III. Título.

CDD 22. ed. 572.865

Bibliotecário(a) responsável: Euzébio Luiz Pinto CRB-6/3317

JÉSSICA RIBEIRO SOARES

Age-dependent miR156-targeted *SPLs* are required for extrafloral nectary development and ecological relationships in *Passiflora* spp.

Thesis submitted to the Plant Physiology Graduate Program of the Universidade Federal de Viçosa in partial fulfillment of the requirements for the degree of *Doctor Scientiae*.

Adviser: Wagner Campos Otoni

APPROVED: March 22, 2024.

Assent:

gov.br Documento assinado digitalmente
JESSICA RIBEIRO SOARES
Data: 28/08/2024 23:17:11-0300
Verifique em https://validar.iti.gov.br

Jéssica Ribeiro Soares

Author

gov.br Documento assinado digitalmente
WAGNER CAMPOS OTONI
Data: 29/08/2024 08:12:43-0300
Verifique em https://validar.iti.gov.br

Wagner Campos Otoni

Adviser

To God.

To my parents.

To the people who believed in me and to those who doubted.

ACKNOWLEDGEMENTS

To God.

To my parents, Pedrelina and Terezino, whose sacrifices and love enabled me to have what they did not have.

To my brothers, that taught me to love my neighbor.

Thanks to Deivid for the companionship, laughter, encouragement, friendship, and support on this journey.

To Elisandra, Lazara, and Lana for their technical support, conversation and laughter, friendship, and making the way easier.

To my advisor, Wagner Otoni, for the trust, friendship, support, and shared knowledge.

To prof. Fabio T. S. Nogueira, for the valuable contributions to this work, and shared knowledge.

To the Tissue Culture Laboratory II (LCT II), for technical support and knowledge exchange. I will carry what I learned throughout my professional career and admire every one of you.

To the Universidade Federal de Viçosa, for the opportunity to complete the postgraduate course and to the Plant Physiology Postgraduate Program Professors.

To the UFV laboratories: Anatomia e Morfogênese de Plantas (DBV/UFV), Bioquímica Genética de Plantas (DBB/BIOAGRO), Genética Molecular de Bactérias (DMB/BIOAGRO), Virologia Vegetal Molecular (DFP/BIOAGRO), Análises Bioquímicas (DBB/BIOAGRO), and the Núcleo de Microscopia e Microanálises (NMM/UFV) and Núcleo de Análise de Biomoléculas (NUBIOMOL/UFV). To Laboratório de Genética e Biotecnologia (ICB/UFJF), Laboratório de Genômica de Plantas e Bioenergia (EEL/USP) and Laboratório de Génetica Molecular do Desenvolvimento Vegetal (ESALQ/USP).

A special thanks to Dr. Fábio G. Faleiro (EMBRAPA Cerrados, Planaltina, DF) and José Rafael da Silva (Viveiro Flora Brasil, Araguari, MG), who kindly donated the seeds used in this work, and to Fundação Otoni de Amparo à Pesquisa (FOAP).

This study was financed in part by the Coordenação de Aperfeiçoamento de Pessoal de Nível Superior – Brasil (CAPES) – Finance Code 001, who granted me the scholarship, and to Fundação de Amparo à Pesquisa do Estado de Minas Gerais (FAPEMIG; grant no. APQ-00772-19).

If I have the gift of prophecy and can fathom all mysteries

and all knowledge, and if I have a faith that can move mountains,

but do not have love, I am nothing.

(1 Corinthians 13:2)

ABSTRACT

SOARES, Jéssica Ribeiro, D.Sc., Universidade Federal de Viçosa, March, 2024. **Age-dependent miR156-targeted *SPLs* are required for extrafloral nectary development and ecological relationships in *Passiflora* spp.** Adviser: Wagner Campos Otoni.

Extrafloral nectaries (EFNs) are recognized as leaf structures that foster important ecologically protective mutualisms between plant and animal communities. In many species, EFNs are absent from leaves produced immediately after germination and appear as the plant ages, indicating a link with plant age. The miR156/*SQUAMOSA PROMOTER BINDING PROTEIN-LIKE* (*SPL*) module is the master regulator of the transition from juvenile to adult vegetative phase, but how age cues control EFN establishment remains poorly understood. Here, we combined genetic and molecular studies to investigate how leaf development and EFN patterning are regulated by miR156/*SPL* module in two EFN-containing *Passiflora* species with distinct leaf shapes. Low miR156 levels correlate with leaf maturation and EFN formation in *Passiflora edulis* and *P. cincinnata*. Consistently, overexpression of miR156 (miR156-OE), leads to low levels of *SPLs*, alters plant height and architecture, leaf morphology, and delayed flowering, as reported in other species. Furthermore, it affected leaf ontogeny and EFN in both species. Laminar EFNs were smaller and less abundant in both *P. edulis* and *P. cincinnata* miR156-OE leaves. Importantly, the ecological relationships established by EFNs and their sugar profiles were negatively regulated by high levels of miR156. Moreover, transcriptome analysis of young leaf primordia revealed that miR156-targeted *SPLs* may be required to properly express leaf and EFN development-associated genes in *P. edulis* and *P. cincinnata*. Our work provides the first evidence that the conserved age-dependent miR156/*SPL* module may be deployed to orchestrate EFN development and that the program responsible for EFN development is closely associated with the heteroblastic developmental program of the EFN-bearing leaves.

Keywords: Vegetative phase change. Nectary. miR156/*SPL*. Passifloraceae. Heteroblasty.

RESUMO

SOARES, Jéssica Ribeiro, D. Sc., Universidade Federal de Viçosa, Março de 2024**. Os genes *SPL*s, regulados pelo miR156, são requeridos para o desenvolvimento do nectário extrafloral e relações ecológicas em *Passiflora* spp.** Orientador: Wagner Campos Otoni.

Os nectários extraflorais (EFNs) são estruturas secretoras foliares que promovem importante interação mutualística de proteção entre as comunidades vegetais e animais. Em muitas espécies, os EFNs estão ausentes nas folhas iniciadas após a germinação e aparecem a medida que a planta envelhece, evidenciando um link com a idade da planta. O módulo miR156/*SQUAMOSA PROMOTER BINDING PROTEIN-LIKE* (*SPL*) é o regulador mestre da mudança de fase vegetativa juvenil para adulta, mas como os sinais de idade controlam o estabelecimento dos EFN permanece pouco compreendido. Aqui, combinamos estudos genéticos e moleculares para investigar como o desenvolvimento foliar e o padrão EFN são regulados através do módulo miR156/*SPL* em duas espécies de *Passiflora* contendo EFN com morfologia foliar distintos. Baixos níveis de miR156 correlacionaram-se com a maturação foliar e formação de EFN em *Passiflora edulis* e *P. cincinnata*. Consistentemente, a superexpressão de miR156 (miR156-OE), que leva a baixos níveis de *SPL*s, promoveram alterações na altura e arquitetura das plantas, morfologia das folhas e atraso na floração, como relatado em outras especies. Além disso, afetou o desenvolviemento foliar e EFN em ambas as espécies. Os EFNs laminares foram menores e menos abundantes nas folhas de *P. edulis* e *P. cincinnata* miR156-OE. Ressalte-se que as relações ecológicas estabelecidas pelos EFNs e o perfil de açúcares foram regulados negativamente por altos níveis de miR156. Além disso, a análise do transcriptoma de primórdios de folhas jovens revelou que *SPLs* alvos a miR156 podem ser necessários para a expressão adequada de genes associados ao desenvolvimento de folhas e EFN em *P. edulis* e *P. cincinnata*. Nosso trabalho fornece a primeira evidência de que o módulo miR156/*SPL* dependente da idade pode ser implantado para orquestrar o desenvolvimento de EFN e que o programa responsável pelo desenvolvimento de EFN está intimamente associado ao programa de desenvolvimento heteroblástico das folhas portadoras de EFN.

Palavras-chave: Mudança de fase vegetativa. Nectário. miR156/*SPL*. Passifloraceae. Heteroblastia.

SUMMARY

General Introduction

After seed germination, plants go through different developmental stages, including juvenile vegetative phase, adult vegetative phase, and reproductive adult phase (Poethig, 2013). The traits associated with the transition from juvenile to adult differ among species and can be accompanied by subtle or conspicuous changes (Yu et al., 2015; Silva et al., 2019; Leichty & Poethig, 2019). These morphological markers generally include changes in leaf morphology and anatomy (heteroblasty), trichome formation, and petiole length (Yu et al., 2010; Silva et al., 2019; Leichty & Poethig, 2019; Lawrence et al., 2021; Poethig & Fouracre, 2024).

The relationship between the vegetative phase transition and phase-specific traits gained significant attention with the discovery of the genetic mechanism orchestrating the vegetative phase transition, including microRNAs and their target genes (Wu et al., 2009; Poethig, 2010; Poethig, 2013). MicroRNAs (miRNAs) are a class of small endogenous RNAs of approximately 20-24 nucleotides that regulate the post-transcriptional expression of target genes by pairing sequences of messenger RNAs (mRNA) that can undergo cleavage and translational repression (Bologna et al., 2018; Wang et al., 2019; Gao et al., 2021). The genes encoding microRNAs are transcribed by RNA polymerase II (Pol II), resulting in the primary transcript pri-miRNAs forming a partially paired hook structure. The pri-miRNAs are recognized and processed by RNase III dicer-like endonucleases (DCLs) and accessory proteins to form miRNA/miRNA* duplexes, which are methylated by the methyltransferase HUA enhancer 1 (HEN1). Only one strand of the duplex (the miR156 guide strand) is assembled with the Argonaute (AGO) protein, while the other is degraded. The miRNA/miRNA* duplexes can remain in the nucleus for cleavage and subsequent assembly of the RNA-induced silencing complex (RISC) or be exported to the cytosol, where RISC loading can also occur. The miRNAs guide the RISC to the target gene for base pairing (fully or partially compatible) and mediate target cleavage or translational inhibition (Wang et al., 2019; Bologna et al., 2018).

MicroRNA156 (miR156) and its target genes *SQUAMOSA PROMOTER BINDING PROTEIN-LIKE* (*SPLs*) are the central regulators of the transition from juvenile to adult vegetative phase. Expression levels of miR156 are elevated in leaves produced early in development and dynamically decrease as more leaves are produced

(Wu et al., 2009; Xu et al., 2016; He et al., 2018; Silva et al., 2009; Xu et al., 2016; He et al., 2018; Silva et al., 2019). In contrast, the expression levels of *SPLs* genes targeted by miR156 have the opposite behavior, acting genes (Wu et al., 2009; Wang et al., 2009; Wang et al., 2019) and, in many processes related to shoot development (Poethig, 2010, 2013; Xu et al., 2016).

The *SPL* genes constitute a multifunctional gene family and have been identified in different plant groups, including bryophytes, lycophytes, gymnosperms, angiosperms, and also in the unicellular alga *Chlamydomonas reinhardtii* (Xu et al., 2016; Guo et al., 2008; Riese et al., 2007; Arazi et al., 2005; Cardon et al., 1999). On the other hand, miR156 has also been conserved during the evolution of land plants, as well as the genetic control performed by the miR156/*SPL* module (Morea et al., 2016; Xu et al., 2016; Arazi et al., 2005).

Constitutive expression of miR156 negatively affects the expression levels of *SPL* target genes. Phylogenetically distinct species with increased miR156 levels, such as *Arabidopsis thaliana*, *Nicotiana tabacum*, *Solanum lycopersicum*, *P. tremula* × *alba*, *Lotus japonicus*, and *Bixa orellana*, showed common phenotypic changes, including alterations in leaf shape and size, plant length, branching index, plant architecture, and delayed flowering time (Wu et al., 2009, Silva et al., 2014, Wang et al., 2015; Feng et al., 2016; Lawrence et al., 2021, Barrera-Rojas et al., 2023 Machado et al., 2023). Other aspects of development, such as sugar metabolism, ovary, and fruit development, stress response, plant defense, and bixin biosynthesis (Yu et al., 2010; Yang et al.,2013; Silva et al., 2014; Arshad et al., 2017; Machado et al., 2023; Ferigolo et al., 2023) are also controlled by the miR156/*SPL* module.

Many species-specific characters are differentially expressed during shoot development. In *Vachellia* species (Fabaceae), structures that characterize the 'swollen thorn syndrome' (presence of beltian bodies, swollen stipular spines, and extrafloral nectaries) are absent at early developmental stages and develop in a mature shoot phase, demonstrating a relationship with vegetative phase changes regulated by the miR156/*SPL* module (Leichty & Poethig, 2019). In these plants, the levels of miR156 and *SPL* target genes were correlated with the manifestation of the syndrome. However, a genetically modified model of the miR156/*SPL* pathway in acacia is not yet available. Interestingly, the absence of extrafloral nectaries in leaves formed shortly after germination and their development in advanced stages of shoot maturation has also

been reported in other species, such as *Passiflora organensis* and *Turnera velutina*, whose formation and complexity of extrafloral nectaries became evident with advancing plant age (Villamil et al., 2013; Moraes et al., 2022).

Nectaries are specialized secretory structures that exude a viscous fluid containing mainly sugars, but also amino acids, proteins, terpenes and phenolics (Heil, 2011; Marazzi et al., 2013, Cardoso-Gustavson et al., 2013). These secretory structures have evolved independently several times in vascular plants and are variable in morphology, anatomy and location (Weber & Keeler, 2013; Brown, 1938). Nectaries can be located on floral organs (floral nectaries - FN) or vegetative organs (e.g. leaf petioles, leaf margins/blade; extrafloral nectaries - EFN). FN attracts pollinators by offering nectar as a reward, thus contributing to the reproductive success of plants (Heil, 2011; Marazzi et al., 2013; Cardoso-Gustavson et al., 2013). On the other hand, EFNs are associated mainly with indirect plant defense and interact with arthropods in a mutualistic manner, providing nectar in exchange for protection (Elias, 1983; Apple & Feener, 2001; Heil, 2015). EFNs have a plethora of effects, such as promoting the longevity and efficiency of entomophagous insects that consume nectar as an energy source, thereby increasing plant fitness (Heil, 2015).

Molecular analyses have shown that the *CRABS CLAW* (*CRC*) gene, a member of the *YABBY* family, plays a key role in the specification and differentiation of the FN in *Arabidopsis* and is necessary for the specification of this structure (Bowman & Smyth, 1999; Lee et al., 2005a). On the other hand, the *CRC* appears not to be involved in the nectary development of *Aquilegia*, a basal eudicot, in which the formation of the FN is under the control of the *STYLISH* (*STY*) genes (Min et al., 2018). Molecular analyses have described many gene families associated with FN formation, including the MADS-box genes, which may be involved in the regulation of *CRC* expression (Lee et al., 2005a; Kram et al., 2009; Morel et al., 2018; Carey et al., 2023).

Despite evidence that EFNs and FNs share the same developmental genetic network (Lee et al., 2005b; Pei et al., 2021), it is possible that EFN formation recruits different regulatory pathways than those required for FNs, and it is likely that nectary development is linked to a pre-existing and active genetic program in the organ that possesses it (Lee et al., 2005b; Krosnick et al., 2011; Marazzi et al., 2013; Leitch & Poethig, 2019).

Genetic and evolutionary analyses of cotton plants exhibiting phenotypes with and without EFNs have suggested that the *GaNEC1* (encoding a PB1 domain-cotaining protein) gene potentially regulates EFN formation in *Gossypium arboreum* (Hu et al., 2020). However, research on the genetic basis regulating the development of EFNs is in its incipient (Leitch & Poethig, 2019; Hu et al., 2020; Pei et al., 2021), and most studies have focused on flower nectaries (Lee et al., 2005 a,b; Kram et al., 2009; Slavković et al., 2020; Carey et al., 2023).

The genus *Passiflora* (Passifloraceae) comprises more than 500 species widely distributed throughout the Neotropics, with a few endemic species in Asia and Oceania. *Passiflora* is divided into subgenera *Decaloba, Astrophaea, Deidamiodes,* and *Passiflora*, with the subgenus *Passiflora* comprising ~250 species, including economically important species (Killip 1938; Ulmer & MacDougal, 2004, Feuillet &MacDougal, 2007). Floral and extrafloral nectaries are common in *Passiflora* species (Cardoso-Gustavson et al., 2013; Lemos et al., 2017; Rocha et al., 2020; Moraes et al., 2022) and can be used as descriptors for taxonomic classification due to their morphological diversity and location (Lemos et al., 2017; Pérez & d'Eeckenbrugge, 2017). *Passiflora* species are an efficient model for studying the genetic mechanisms that control the formation of floral or extrafloral nectaries, whether these are private or shared genetic programs.

Passiflora edulis and *Passiflora cincinnata* are perennial climbing species of the subgenus *Passiflora* with EFNs located on the petiole (petiolar EFN) and leaf margin (laminar EFN). In both species, the presence and abundance of nectaries is associated with changes in leaf morphological pattern (leaf heteroblasty) (Chitwood & Otoni, 2017 a, b; Silva et al., 2019), which in turn is associated with the change from juvenile to adult phase in *Passiflora* (Silva et al., 2019). Interestingly, both the change from juvenile to adult vegetative phase and leaf heteroblasty are under the regulation of the miR156/*SPL* module (Wu et al., 2009; Feng et al., 2016; Poethig, 2013; Silva et al., 2019; Machado et al., 2023). In this study, we investigated whether EFN development in two different *Passiflora* species (*P. edulis* and *P. cincinnata*) is under the control of the miR156/*SPL* module.

References

Apple JL, Feener DH. 2001. Ant visitation of extrafloral nectaries of *Passiflora*: The effects of nectary attributes and ant behavior on patterns in facultative ant-plant mutualisms. *Oecologia* **127**: 409–416

Arazi T, Talmor-Neiman M, Stav R, Riese M, Huijser P, Baulcombe DC. 2005. Cloning and characterization of micro-RNAs from moss. *The Plant Journal* ***43*****(6):** 837-848.

Arshad M, Feyissa BA, Amyot L, Aung B and Hannoufa A. 2017. MicroRNA156 improves drought stress tolerance in alfalfa (*Medicago sativa*) by silencing *SPL13*. *Plant Science* **258**: 122–136.

Barrera-Rojas CH, Vicente MH, Brito DAP, Silva EM, Lopez AM, Ferigolo LF, Carmo RMD, Silva CMS, Silva GFF, Correa JPO, Notini MM, Freschi L, Cubas P, Nogueira FTS. 2023. Tomato miR156-targeted SlSBP15 represses shoot branching by modulating hormone dynamics and interacting with GOBLET and BRANCHED1b**.** *Journal of Experimental Botany* **74(17)**: 5124–5139.

Bologna NG, Iselin R, Abriata LA, Sarazin A, Pumplin N, Jay F, Grentzinger T, Dal Peraro M, Voinnet O. **2018.** Nucleo-cytosolic shuttling of *ARGONAUTE1* prompts a revised model of the plant microRNA pathway. *Molecular Cell* **69 (4)**:709-719.e5.

Bowman JL, Smyth DR.1999. *CRABS CLAW*, a gene that regulates carpel and nectary development in *Arabidopsis*, encodes a novel protein with zinc finger and helix-loop-helix domains. *Development* **126:** 2387–2396.

Brown W H. 1938. The bearing of nectaries on the phylogeny of flowering plants. *Proceedings of the American Philosophical Society*, 549-595.

Cardon G, Höhmann S, Klein J, Nettesheim K, Saedler H, Huijser P. 1999. Molecular characterisation of the Arabidopsis SBP-box genes. *Gene* **237(1):** 91-104.

Cardoso-Gustavson P, Andreazza NL, Sawaya ACHF, Castro MM. **2013**. Only Attract Ants? The Versatility of Petiolar Extrafloral Nectaries in *Passiflora*. *American Journal of Plant Sciences* **4**: 460–469

Chitwood DH, Otoni WC. **2017a.** Morphometric analysis of *Passiflora* leaves: the relationship between landmarks of the vasculature and elliptical Fourier descriptors of the Blade. *GigaScience* **6(1)**: giw008

Chitwood DH, Otoni WC. **2017b**. Divergent leaf shapes among *Passiflora* species arise from a shared juvenile morphology. *Plant Direct* **1(5)**: e00028

Elias TS. 1983. Extrafloral nectaries: their structure and distribution. *The biology of nectaries*. In: Bentley, B.L. and Elias, T.S., Eds. The Biology of Nectaries, Columbia University Press, New York, 174-203.

Feng S, Xu Y, Guo C, Zheng J, Zhou B, Zhang Y, Ding Y, Zhang L, Zhu Z, Wang H, Wu G. 2016. Modulation of miR156 to identify traits associated with vegetative phase change in tobacco (*Nicotiana tabacum*). *Journal of Experimental Botany* **67**: 1493–1504

Ferigolo LS, Vicente MH, Correa JPO, Barrera-Rojas CH, Silva EM, Silva GFF, Carvalho Jr A, Peres LEP, Ambrosano GB, Margarido GRA, Sablowski R, Nogueira FTS. 2023. Gibberellin and the miRNA156-targeted SlSBPs synergistically regulate tomato floral meristem determinacy and ovary patterning. *Development* **150(21):** dev201961.

Feuillet C, MacDougal M. 2007. Passifloraceae. In: Kubitzki K (Eds) Flowering Plants Eudicots. The families and genera of vascular plants. Springer, Berlin, Heidelberg **9**:270–281

Gao Z, Nie J, Wang H. 2021. MicroRNA biogenesis in plant. *Plant Growth Regul*ation **93**: 1–12

Guo AY, Zhu Q H, Gu X, Ge S, Yang J, Luo J. 2008. Genome-wide identification and evolutionary analysis of the plantspecific SBP-box transcription factor family. *Gene* **418(1-2)**: 1-8

He J, Xu M, Willmann MR, McCormick K, Hu T, Yang L, Starker CG, Voytas DF, Meyers BC, Poethig RS. 2018. Threshold-dependent repression of *SPL* gene expression by miR156/miR157 controls vegetative phase change in *Arabidopsis thaliana*. *PLoS Genetics* **14**: e1007337

Heil M. 2011. Nectar: generation, regulation and ecological functions. *Trends in Plant Science* **16(4)**: 191-200.

Heil M. 2015. Extrafloral nectar at the plant-insect interface: a spotlight on chemical ecology, phenotypic plasticity, and food webs. *Annual Review of Entomology* **60**: 213-232

Killip EP. 1938. The American species of Passifloraceae. *The American species of Passifloraceae.*, 407:407-408

Kram B W, Xu WW, Carter CJ. 2009. Uncovering the *Arabidopsis thaliana* nectary transcriptome: investigation of differential gene expression in floral nectariferous tissues. *BMC Plant Biology* **9:**92.

Lawrence EH, Leichty AR, Doody EE, Ma C, Strauss SH, Poethig RS. 2021. Vegetative phase change in *Populus tremula* x *alba*. *New Phytologist* **231**:351−64

Lee J Y, Baum SF., Alvarez J, Patel A, Chitwood D H, Bowman JL. 2005a. Activation of *CRABS CLAW* in the nectaries and carpels of Arabidopsis. *The Plant Cell* **17(1)**: 25-36.

Lee JY, Baum SF, Oh SH, Jiang CZ, Chen JC, Bowman JL. **2005b**. Recruitment of *CRABS CLAW* to promote nectary development within the eudicot clade. *Development* **132**: 5021–5032

Leichty AR, Poethig RS. 2019. Development and evolution of age-dependent defenses in ant-acacias. *Proceedings of the National Academy of Sciences, USA*, **116**: 15596–15601.

Lemos RCC, Costa Silva D, Albuquerque Melo-de-Pinna GF. **2017**. A structural review of foliar glands in *Passiflora* L. (Passifloraceae). *PLoS ONE* **12(11):** e0187905.

Macêdo LPM, Silva EO, Aguiar-Dias ACA. **2021**. Morphoanatomy and ecology of the extrafloral nectaries in two species of *Passiflora* L. (Passifloraceae). *South African Journal of Botany* **143**: 248–255.

Machado KLG, Faria DV, Duarte MBS, Silva LAS, Oliveira TR, Falcão TCA, Batista DS, Costa MGC, Santa-Catarina C, Silveira V, Romanel E, Otoni WC, Nogueira FTS. 2023. Plant age-dependent dynamics of annatto pigment (bixin) biosynthesis in *Bixa orellana* L. *Journal of Experimental Botany* **17**:erad458.

Marazzi B, Bronstein JL, Koptur S. 2013. The diversity, ecology and evolution of extrafloral nectaries: current perspectives and future challenges. *Annals of Botany* **111(6)** 1243-1250.

Min Y, Bunn J I, Kramer EM. 2019. Homologs of the STYLISH gene family control nectary development in *Aquilegia*. *New Phytologist* **221(2)**: 1090-1100.

Moraes TS, Rossi ML, Martinelli AP and Dornelas MC. 2022. Morphological and anatomical traits during development: Highlighting extrafloral nectaries in *Passiflora organensis*. *Microscopy Research Technique* **85**: 2784–2794

Morea EGO, da Silva EM, e Silva GFF, Valente GT, Barrera Rojas CH, Vincentz M, Nogueira FTS. 2016. Functional and evolutionary analyses of the miR156 and miR529 families in land plants. *BMC Plant Biology* **16**:40

Pei Y, Zhang J, Wu P, Ye L, Yang D, Chen J, Li J, Hu Y, Zhu X. **2021** GoNe encoding a class VIIIb *AP2 / ERF* is required for both extrafloral and floral nectary development in Gossypium. *The Plant Journal* **106**:1116–1127

Pérez JO, d'Eeckenbrugge GC. 2017. Morphological characterization in the genus *Passiflora* L.: an approach to understanding its complex variability. *Plant Systematics and Evolution* **303**: 531–558

Poethig RS, Fouracre J. 2024. Temporal regulation of vegetative phase change in plants. *Developmental Cell* **59(**1): 4–19

Poethig RS. 2010. The Past, Present, and Future of Vegetative Phase Change. *Plant Physiology* **154(2)**: 541–544

Poethig RS. **2013**. Vegetative phase change and shoot maturation in plants. *Current Topics in Developmental Biology* **115**:125–152

Riese M, Höhmann S, Saedler H, Münster T, Huijser P. 2007. Comparative analysis of the SBP-box gene families in *P. patens* and seed plants. *Gene* **401(1-2):** 28-37.

Rocha DI, Batista DS, Faleiro FG, Rogalski M, Ribeiro LM, Mercadante-Simões MO, Yockteng R, Silva ML, Soares WS, Pinheiro MVM, Pacheco TG, Lopes AS, Viccini LF, Otoni, WC. **2020.** Passion Fruit: *Passiflora* spp. In: Litz, R.A.; Pliego-Alfaro, F.; Hormaza, J.I. (eds) Biotechnology of Fruit and Nut Crops, 2nd Edition, CABI, Wallingford, UK. Pp 381 402.

Silva GFFE, Silva EM, Da Silva Azevedo M, Guivin MAC, Ramiro DA, Figueiredo CR, Carrer H, Peres LEP, Nogueira FTS. **2014**. MicroRNA156-targeted *SPL/SBP* box transcription factors regulate tomato ovary and fruit development. *The Plant Journal*, **78**: 604–618

Silva PO, Batista DS, Cavalcanti JHF, Koehler AD, Vieira LM, Fernandes AM, Barrera-Rojas CH, Ribeiro DM, Nogueira FTS, Otoni WC. **2019**. Leaf heteroblasty in *Passiflora edulis* as revealed by metabolic profiling and expression analyses of the microRNAs miR156 and miR172. *Annals of Botany* **123**: 1191–1203

Ulmer T, MacDougal J M. 2004. *Passiflora*: Passionflowers of the world. Timber Press.

Villamil N, Márquez-Guzmán J, Boege K. 2013. Understanding ontogenetic trajectories of indirect defence: ecological and anatomical constraints in the production of extrafloral nectaries. *Annals of Botany* **112 (4)**: 701–709.

Xu M, Hu T, Zhao J, Park M-Y, Earley KW, Wu G, Yang L, Poethig RS. **2016**. Developmental Functions of miR156-Regulated *SQUAMOSA PROMOTER BINDING PROTEIN-LIKE* (*SPL*) Genes in *Arabidopsis thaliana*. *PLOS Genetics* **12**: e1006263

Wu G, Poethig RS. 2006. Temporal regulation of shoot development in Arabidopsis thaliana by miR156 and its target *SPL*3.

Wu G, Park MY, Conway SR, Wang JW, Weigel D, Poethig RS. 2009. The sequential action of miR156 and miR172 regulates developmental timing in *Arabidopsis*. *Cell* **138**: 750–759

Wang JW, Czech B, Weigel D. 2009. miR156-Regulated *SPL* Transcription Factors Define an Endogenous Flowering Pathway in *Arabidopsis thaliana*. Cell **138:** 738–749

Wang J, Mei J, Ren G. 2019. Plant microRNAs: biogenesis, homeostasis, and degradation. *Frontiers in plant science* **10:** 360.

Wang Y, Wang Z, Amyot L, Tian L, Xu Z, Gruber MY, Hannoufa A. 2015. Ectopic expression of miR156 represses nodulation and causes morphological and developmental changes in *Lotus japonicus*. *Molecular Genetics and Genomics* **290**: 471–484

Wang L, Zhou CM, Mai YX, Li LZ, Gao J, Shang GD, Lian H, Han L, Zhang TQ, Tang HB, Ren H, Wang FX, Wu LY, Liu XL, Wang CS, Chen EW, Zhang XN, Liu C, Wang JW. 2019. A spatiotemporally regulated transcriptional complex underlies heteroblastic development of leaf hairs in *Arabidopsis thaliana*. EMBO Journal. **238(8)**:e100063.

Weber M G, Keeler KH. 2013. The phylogenetic distribution of extrafloral nectaries in plants. *Annals of Botany* **111(6):** 1251-1261.

Yu S, Lian H, Wang JW. 2015. Plant developmental transitions: The role of microRNAs and sugars. *Current Opinion Plant Biology* **27**: 1–7

Yu N, Cai WJ, Wang S, Shan CM, Wang LJ, Chena XY. **2010**. Temporal control of trichome distribution by microRNA156-targeted *SPL* genes in *Arabidopsis thaliana*. *The Plant Cell* **22**: 2322–2335

1. Introduction

Plants evolved versatile adaptive strategies to different environments and underwent several developmental transitions during their life cycle. The transition from juvenile to adult vegetative phase can be accompanied by changes in leaf traits, including the formation of secretory structures (Leichty & Poethig, 2019). In many plant species, the development or increase in the abundance of extrafloral nectaries (EFNs) occurs as the plant ages (Villamil et al., 2013; Kwok & Laird, 2012; Leichty & Poethig, 2019; Moraes et al., 2022). For example, the abundance and complexity of EFNs increase in *Turnera velutina* as the plant progresses into the reproductive phase (Villamil et al., 2013). In *Passiflora organensis,* EFNs are absent in the juvenile vegetative stage, with the adult stage characterized by EFN formation on the abaxial side of the leaf lamina (Moraes et al., 2022).

As secretory structures, nectaries secrete a chemically complex compound called nectar, which is rich in carbohydrates but can also contain amino acids, proteins, alkaloids and phenolics (Heil, 2011; Marazzi et al., 2013, Cardoso-Gustavson et al., 2013). Floral nectaries (FNs) are found in the floral whorls and, together with floral morphology, support a co-evolutionary relationship with pollinators (Ulmer & MacDougal, 2004; Pérez & d'Eeckenbrugge, 2017). On the other hand, EFNs are located on leaves, leaf petioles, stipules or floral bracts and play a role in the indirect defense of plants by attracting insects, primarily ants, which protect the plant from herbivore attacks in exchange for nectar, establishing a mutualistic interaction (Elias, 1983, Apple & Feener, 2001; Heil, 2015). EFNs have a plethora of effects reflected in the increased longevity and efficiency of entomophagous insects that consume nectar as an energy source and increased crop productivity by contributing to reduced herbivory (Heil, 2015).

Recent investigations into the genetic basis of nectary development have provided evidence that FNs and EFNs share developmental genetic networks (Lee et al., 2005; Pei et al., 2021). However, it is important to consider that the EFN development may recruit different regulatory pathways than those required for FNs (Marazzi et al., 2013). Nectary development is thought to be regulated by the same genetic program that is present and active in the organ that has this secretory structure (Lee et al., 2005; Marazzi et al., 2013; Leichty & Poethig, 2019). For example, changes in the morphology of EFNs present in the main vein of leaves of *Gossypium arboreum* have

been shown to accompany leaf ontogeny (Hu et al., 2020). Although the *CRABS CLAW* (*CRC*) gene has been recognized as an important regulator of FN development in distinct species such as *G. hirsutum* and *Petunia hybrida* (Lee et al., 2005), the underlying mechanisms regulating the development and growth of EFNs are poorly understood, as most genetic and molecular studies have focused on FNs.

The genus *Passiflora* is represented by more than 500 species distributed in four subgenera: *Passiflora*, *Decaloba*, *Astrophaea*, and *Deidamiodes*, with the subgenus *Passiflora* being the most representative of the genus (Killip, 1938; Ulmer & MacDougal, 2004; Feuillet &MacDougal, 2007; Pérez & d'Eeckenbrugge, 2017). Floral and extrafloral nectaries are common in many *Passiflora* species, making the genus relevant for studies on the evolution, development and ecology of nectaries and nectar metabolites (Apple & Feener, 2001; Rocha et al., 2009; Cardoso-Gustavson et al., 2013; Pérez & d'Eeckenbrugge, 2017; Lemos et al., 2017; Moraes et al., 2022). Comparative analyses of EFN patterning suggest a shared developmental program with leaf development to create EFN diversity in *Passiflora* species. Importantly, EFN final location and morphology depend on the maturity of the leaf tissue where the shared program is active (Krosnick et al., 2011).

Passiflora edulis and *P. cincinnata* are perennial climbing vines, in which EFNs are located adaxially in the petiole (petiolar EFN) and abaxially on the leaf margin (laminar EFN). Petiolar EFNs in *P. edulis* are present in monolobed and trilobed leaves, corresponding to the juvenile and adult vegetative phases, respectively (Silva et al., 2019), whereas laminar EFNs are only observed in the adult phase. In contrast, *P. cincinnata* petiolar and laminar EFNs are observed in trilobed leaves during the juvenile vegetative phase and remains in the adult phase, when the leaves become five-lobed. These gradual changes in leaf patterning during the transition from juvenile to adult phase are known as leaf heteroblasty and have been documented for many species in the genus *Passiflora* (Chitwood & Otoni, 2017 a, b; Silva et al., 2019).

MicroRNA156 (miR156) is a key regulator of the transition from the juvenile to the adult vegetative phase in species of different families. The expression levels of miR156 are gradually reduced as the adult phase is established, while the expression levels of its targets, the *SQUAMOSA PROMOTER-BINDING PROTEIN-LIKE* (*SPL*) family of transcription factors, increase, promoting adult vegetative traits and flowering competence (Wu et al., 2009; Xu et al., 2016; He et al., 2018; Silva et al., 2019; Poethig & Fouracre, 2024). The miR156/*SPL* module is highly conserved among angiosperms.

It has been extensively studied in multiple processes of plant development, including leaf morphology and maturation, trichome development, sugar metabolism, axillary bud initiation, shoot architecture, fruit development, stress responses, plant defense and bixin biosynthesis (Wu et al., 2009; Yu et al, 2010; Poethig, 2013; Silva et al., 2014; Feng et al., 2016; Arshad et al., 2017; Guo et al., 2017; Silva et al., 2019; Fouracre & Poethig, 2019; Lawrence et al., 2021; Machado et al., 2023; Barrera-Rojas et al., 2023; Ferigolo et al., 2023). Leaf heteroblasty in *P. edulis* was correlated with the dynamic expression patterns of miR156 and *PeSPL9* (Silva et al., 2019), suggesting that the miR156/*SPL* module can regulate leaf maturation in *Passiflora*. In addition, the development of the swollen thorn syndrome in *Vachellia* species,was correlated with a decrease in miR156 transcripts and increased expression of miR156-targeted *SPLs* (Leichty & Poethig, 2019). However, how the miR156/*SPL* module regulates leaf traits such as the establishment of EFNs or the swollen thorn syndrome is unclear.

The objective of this work was to study the development of EFNs in two species of *Passiflora* (*P. edulis* and *P. cincinnata*) which exhibit distinct leaf morphology and answer the following question: miR156/*SPL* module modulates the development of EFNs through the leaf ontogeny?

2. Materials and Methods

2.1 Generation of microRNA156 overexpression lines in *Passiflora cincinnata* Mast. and *Passiflora edulis* Sims.'

Seeds of *Passiflora cincinnata* Mast. cv. BRS 'Sertão Forte' and *Passiflora edulis* Sims. 'FB-300' were kindly donated by Dr. Fábio Gelape Faleiro (EMBRAPA Cerrados, Brazil) and Viveiros Flora Brazil Ltda. (Araguari, MG, Brazil), respectively. The seeds were mechanically decoated and were surface-sterilized in 70% ethanol, for 60 s, under a laminar flow hood. Following, immersed in a commercial sodium hypochlorite solution – 2.0-2.5% active chlorine plus two drops of Tween 80 (for each 100 mL of bleaching solution), for 15 min. The material was rinsed thrice (30 s duration each) with sterile water. Approximately ten decoated seeds of *P. edulis* and *P. cincinnata* were inoculated in each bottle (250 mL capacity) containing 50 mL of MS medium containing MS basal salts and vitamins (Murashige and Skoog, 1962) (PhytoTech® Labs, Kansas), 0.01% (w/v) myo-inositol (Sigma Chem. Co., St Louis), 3.0% (w/v) sucrose (PhytoTech® Labs), and 0.6% (w/v) agar (Plant TC Micropropagation Grade; (PhytoTech® Labs). The pH of the medium was adjusted to 5.8 ± 0.05 before adding the gelling agent and, autoclaved at 121 ℃, 108 kpa, for 20 min.

To optimize gas exchange, the bottles were closed with polypropylene caps with two holes (10 mm) covered with 0.45 μm porous membranes (Milliseal®, AVS-0.45 Air Vent, Japan). Seeds were kept for 15 days in the dark, at 25 ± 1 °C, followed by 15 days under a 16-h photoperiod and irradiance of 50 ± 3 μmol m^{-2} s^{-1}.

Genomic fragment harboring the *AtMIR156a* precursor was amplified from *Arabidopsis thaliana* as described Feng et al. (2016). *Agrobacterium tumefaciens* strain AGL-1 with a miR156 overexpression construct (p35S: HygR pUbi10-MIR156a-AtuOCS pMAS-CRT1) was cultivated in liquid LB medium containing 50 mg L^{-1} rifampicin (PhytoTech® Labs) and 100 mg L^{-1} kanamycin (PhytoTech® Labs), and carbenicillin (Gibco, Grand Island, NY) for 48 h at 28 °C and 120 rpm. The inoculum was used when the bacterial culture's optical density (OD_{600} nm) reached values of 0.45-0.5. Then it was centrifuged at 3,500 *g* for 10 min. The pellet was resuspended in MS liquid medium, and supplemented with 30 g L^{-1} of sucrose and myo-inositol for an OD_{600} nm of 0.5. Ten minutes before inoculation, sterile acetosyringone (Acros Organics, Morris Plains, NJ) 100 μM was added to the bacterial suspension.

The transformation protocol was modified according to Manders et al. (1994) and Otoni et al. (2007). Thirty-d-old seedlings (15 days dark/15 days light) were used as a source of explants. Hypocotyls were sectioned transversally in segments of 0.8 – 1.0 cm in the suspension of *A. tumefaciens*, and after 15-20 min, the excess suspension was discarded. The explants were transferred to the regeneration medium composed of MS salts and vitamins supplemented with 3.0% (w/v) sucrose, 100 mg L^{-1} myo-inositol, 1 mg L^{-1} 6-benzylaminopurine (BA; PhytoTech Labs®) and 100 μM acetosyringone, starting the co-culture stage under dark conditions at 25°C, for two days. After, the explants were triple rinsed with liquid MS medium containing 300 mg L^{-1} of Timentin (PhytoTech® Labs), and 250 mg L^{-1} Cefotaxime (PhytoTech Labs®). Subsequently, it was transferred to the semi-solid MS-based selective medium, with BA 1 mg L^{-1}, hygromycin (PhytoTech Labs®) at 6 mg L^{-1}, Norflurazon (Sigma Chem. Co.) at 3.8 mg L^{-1}, and Timentin at 300 mg L^{-1}. Explants were kept at 25 ± 1 °C under a photoperiod of 16:8 h and irradiance of 50 ± 3 μmol m^{-2} s^{-1} for six weeks, and every 15 days recultured to a freshly prepared selective culture. In the elongation phase, well-developed shoots (above 0.5 mm) were transferred to flasks containing hormone-free MS medium supplemented with hygromycin and Norflurazon.

2.2 Plant growth conditions

Non-transgenic (NT) plantlets and two independent miR156-overexpressing lines of *P. edulis* (*Pe*OE-3 and *Pe*OE-5) and *P. cincinnata* (*Pc*OE-1 and *Pc*OE-4) were subcultured monthly on MS-based medium without growth regulators. Then, for initial acclimatization, the plants were transferred to 150 ml disposable cups containing horticultural soil conditioner substrate (Tropstrato® HT Hortaliças, Vida Verde Indústria e Comércio de Insumos Orgânicos Ltda, Mogi Mirim, SP, Brazil), and kept in a growth room with a photoperiod of 16 h, irradiance of 50 μmol $m^{-2}s^{-1}$ and temperature of 25 ± 1 °C for two weeks. The plants were transferred to 5-L polyethylene pots with Tropstrato® HT, and maintained under greenhouse conditions at Universidade Federal de Viçosa (20º 45’ S, 42º 15’ W), Viçosa, MG, Brazil. The fertilizer Osmocote® Plus 16-08-12 (5-6M) (ICL, USA) was added (2 g per pot) bimonthly. The plants were watered daily and maintained at an 11/13-h light/dark photoperiod and 25/16 °C (day/night).

Access to genetic heritage adhered strictly to current Brazilian biodiversity legislation and was approved by the Brazilian National System for the Management of Genetic Heritage and Associated Traditional Knowledge (SISGEN) under permission number AF1B74A. All GMO manipulations were performed in the Laboratório de Cultura de Tecidos II – Bioagro and in a GMO-adapted greenhouse following the CTNBio and CIBio-UFV biosafety rules (CQB 024/97, CTNBio nº 19, process number 01200.002610/9704).

2.3 Confirmation of insert introduction through Polymerase chain reaction (PCR)

To confirm the transgenic lines the presence of the *hptII* gene was assessed by PCR using genomic DNA. The genomic DNA was extracted from fully expanded leaves according to the Doyle & Doyle (1987) method, with the addition of 2% polyvinylpyrrolidone to the CTAB buffer. DNA integrity and quality verified by 1.5% agarose gel electrophoresis, and quantified using a NanoDrop™ Lite spectrophotometer (Thermo Scientific, Wilmington, DE, USA). RNA was digested using Rnase A (Sigma-Aldrich) according to the manufacturer's instructions. PCR configuration as been performed according to the user's manual. Platinum™ II Taq Hot-Start DNA Polymerase (Invitrogen™, Thermo Scientific). The primers used for the PCR are shown in Supplementary Table 1 (Table S1).

2.4 Flow cytometry analysis

Genetic stability of lines miR156-OE was evaluated by assessing the relative DNA content from plants after 120 days grown in green house. Briefly cell nuclei suspensions were prepared by cutting approximately 20-30 mg of young leaves from the samples and the internal reference (*Pisum sativum* 'Citrad', 2C = 9.09 pg) and mixed with 1 mL of WPB isolation buffer (Doležel et al.,1998; Loureiro et al., 2007). The generated suspension was filtered through a nylon membrane (50 µm mesh) and 25 µL of propidium iodide solution (1 mg mL^{-1}; Sigma-Aldrich, St. Louis, MO, USA) and 5 mL RNAse (Amresco, Framingham, MA, USA) were added to each sample that were incubated in the dark for 1 h. The analysis was performed using a CytoFLEX flow cytometer (Beckman Coulter, CA, USA). Three replicates were used, and fluorescence was quantified in at least 10,000 nuclei. Histograms were generated and analyzed using CytExpert 2.0 (Beckman-Coulter) and DNA content (pg) was calculated according to the formula proposed by Doležel & Bartoš (2005).

2.5 Analyses of growth parameters

The main branch height (cm), internode length fourth to fifth leaf (shootwards) and branching index of plants (ratio between the total length of lateral ramification and the length of the main plant axis; Morris et al., 2001) were assessed after 35 and 60 days of growth after transfer to greenhouse conditions for *P. edulis* and *P. cincinnata*, respectively.

2.6 Number, size and ants visitation of extrafloral nectaries (EFNs)

The number of petiolar and laminar EFNs from fully expanded leaves was determined, considering fourth (4^{th}) and sixteenth (16^{th}) phytomer for *P. edulis*, and fourth (4^{th}) twelfth (12^{th}) phytomer for *P. cincinnata*. To determine the size, the nectaries were photographed in a stereomicroscope (Olympus SZX7 - Olympus Corporation, Tokyo- Japan) and had the diameter (mm) and area (length x width- mm^2) quantified using ImageJ software v.1.43u (National Institutes of Health, USA) (Schneider et al., 2012). During the greenhouse experiment, we monitored the presence of an ant species that patrolled naturally the *Passiflora* plants. We then determined the total number of ants visiting each NT and miR156-OE plants of *P. edulis* and *P. cincinnata* at noon for 10 days (Izaguirre et al., 2013). The number of ants per plant was determined by the ratio between the total number of ants present on the plant per day and the total number of branches larger than 1 cm. The plants were completely randomized and 8-9 plants for NT and miR156-OE of both *Passiflora* species were sampled. To better understand the relationship between the observed patrolling ant and the *Passiflora* species, the genus of the ant species was identified.

2.7 Histological analyses and scanning electron microscopy (SEM)

Petiolar and laminar EFNs were fixed in Karnovsky (Karnovsky, 1965) from fully expanded leaves considering sixteenth (16^{th}) phytomer for *P. edulis*, and twelfth (12^{th}) phytomer for *P. cincinnata*; and dehydrated in graded ethanol series (10-100%) and included in methacrylate (Historesin®, Leica Instruments, Germany). Sections (5 µm) were obtained using automatic feed rotary microtome (RM2155, Leica Instruments, Germany) and stained in toluidine blue (pH 4.7) for 2 min (O'Brien & McCully, 1981). The slides were mounted in Permount® SP15-500 (Fisher Scientific, Waltham) and observed under a light microscope (AX70 TRF, Olympus Optical) with U-photo system, coupled to a digital camera (Spot Insightcolour 3.2.0, Diagnostic

Instruments Inc.). For SEM, samples were fixed in Karnovsky, submitted dehydration in ethylic series, and dried at the critical point, utilizing CO_2 in Balzers equipment (model CPD 020, Bal-Tec, Balzers, Liechtenstein). Subsequently, the fragments were covered in gold using the cathodic spraying process in Sputter Coater equipment (Model FDU 010, Bal-Tec, Balzers, Liechtenstein) (Silveira, 1989). The observations and photographic documentation were carried out using a scanning electron microscope (model Leo 1430 VP, Zeiss, Cambridge, England). The number of cells constituting the nectary epidermis and parenchyma (nectariferous and subnectariferous parenchyma) was determined using Image J software (Schneider et al., 2012).

2.8 Total RNA extraction

Leaf primordia were collected from the 16th and 12th phytomer of *P. edulis* and *P. cincinnata* respectively. Total RNA was extracted from 50 mg of macerated leaf tissue using the Trizol method, according to the manufacturer's instructions (TRIzol™ Reagent – Invitrogen). RNA quantification was performed with the aid of NanoDrop™ Lite (Thermo Scientific, Wilmington, DE) under an absorbance of 260 nm, and the integrity of the RNA samples was verified by 1.5% agarose gel electrophoresis (RNAse free). Samples were then treated with DNAse (RQ1 RNAse-Free DNAse-Promega), according to the manufacturer's instructions.

2.9 Library Preparations and RNA sequencing

Total RNA and Dynabeads® Oligo (dT) 25 (Thermo Fisher Scientific, Waltham, MA, USA) were used to isolate mRNA. The resulting mRNA fragments of ~400 nucleotides were converted to double-stranded complementary DNA (cDNA) using random hexamer primers and corresponding enzymes following standard DNA library protocols for sequencing. Briefly, cDNA was end-repaired, phosphorylated, and adenylated. Common TruSeq adapters containing 8-bp indexes (i5 and i7) suitable for Illumina sequencing were then ligated to the adenylated molecules, and the resulting libraries were amplified by 13 cycles of PCR to enrich for properly ligated molecules. The final libraries were quantified using PicoGreen (Thermo Fisher Scientific) and equally combined into a single sample, then sequenced on an Illumina HiSeq X (Illumina Inc., San Diego, CA, USA) instrument. Paired-end reads with an average length of 150 bp were obtained. Library preparation and sequencing were carried out by Rapid Genomics, LLC (Gainesville, FL, USA).

2.10 *De novo* assembly and annotation

For each genotype, three and four RNA libraries were sequenced for *P. edulis* and *P. cincinnata*, respectively. Trimmomatic software v 0.39 removed adapters and reads with phred score quality less than Q20. All cleaned reads from each pair-end were pooled and assembled using Trinity software version 2.11.0 with default parameters. The coding DNA sequence (CDS) was predicted using transdecoder v5.5.0 software (https://github.com/TransDecoder/TransDecoder) with default parameters. For the transcriptome assessment, we used BUSCO (Benchmarking Universal Single-Copy Orthologs) (Manni et al., 2021).

All assembled transcripts and predicted ORFs were annotated against Swiss-prot, Uniref 50, Uniref90, Pfam, EggNOG, Gene Ontology (GO) databases using trinotate pipeline. For BLASTp search, we used a cut-off e-value of 1.0E-3. All results were deposited into SQLite database, and a spreadsheet summary report was generated. To quantify the gene expression level of all samples, we performed mapping clean reads to assembled transcripts using the salmon v 0.14.1 program. From this abundance estimation, we used the DESeq2 v1.36.0 R package to carry out the differential expression analysis of gene and transcript level of trinity software. Heatmap and volcano were plotted in R v 3.5.1. GO enrichment analysis of a subset of DEGs ($p < 0.05$) was conducted using Goseq, GO.db, and qvalue packages from R with default parameters.

2.11 Identification, phylogenetic and sequence analysis of *Passiflora SPL* gene family

To identify the sequences containing the SBP/*SPL* domain (PF03110), all 58087 transcripts generated by RNA from *P. edulis* and 71034 from *P. cincinnata* annotated against the Swiss-prot database were used. Transdecorder predicted a total of 112 sequences of *SPL* genes for *P. edulis* and 90 sequences for *P. cincinnata*, which were used as a query to conduct BLASTx in the NCBI (National Center for Biotechnology Information) database. 11 *SPL* family genes in *P. edulis* and 11 in *P. cincinnata* were selected considering the high identity and coverage of the sequences.

All retrieved CDS were translated in all six frames using EMBOSS Transeq (https://www.ebi.ac.uk/Tools/st/emboss_transeq/) and analyzed by PFAM v35.0 (Salazar et al., 2020) to maintain only those containing the SBP/*SPL* domain

(Supplementary Table S4). All unique and primary coding sequences from *Solanum lycopersicum* (ITAG4.0 assembly), *Populus trichocarpa* (v4.1 assembly), *Vitis vinifera* (v2.1 assembly), and *Panicum virgatum* (v4.1 assembly) were downloaded at Phytozome v13 and used to recovery sequences containing PF03110 domain. The name of SBP or *SPL* gene names were used as described previously for *Arabidopsis* (Preston & Hileman, 2013), tomato (Salinas et al., 2012), poplar (Guo et al., 2021; Hou et al., 2013), grapes (Hou et al., 2013; Díaz-Riquelme et al., 2012), and switchgrass (Wu et al., 2016).

All protein sequences for each multigene family were aligned using the default settings of Multiple Sequence Comparison by Log-Expectation (MUSCLE) (http://www.ebi.ac.uk/Tools/msa/muscle/; Madeira et al., 2022). A Maximum Likelihood (ML) phylogenetic analysis was performed as using PhyML3.0 (Guindon et al., 2010), using Smart Model Selection (SMS) to select the best model (Lefort et al., 2017) (like VT+R+F substitution model), and aLRT branch support testing (Anisimova & Gascuel, 2006). The phylogenetic tree was visualized using the iTOL software (https://itol.embl.de; Letunic & Bork, 2021). High-confidence prediction of miRNA156 targets in *P. edulis* was performed by psRNATarget (Dao & Zhao, 2011) using the database https://www.zhaolab.org/psRNATarget/analysis. We have used a strict cut-off threshold for the Maximum Expectation (E) parameter (range 0 - 3.0).

2.12 Analysis of gene expression by RT-qPCR

For microRNA quantification, we used the stem-loop qPCR protocol previously described by Varkonyi-Gasic et al. (2007). For the remaining genes, cDNA was synthesized using the SuperScript III First-Strand Synthesis System for the RT-PCR kit (Invitrogen, San Diego, CA), according to the manufacturer's instructions. PCR reactions were performed using iTaq Universal SYBR Green supermix (Bio-Rad) and analyzed in a Step-OnePlus real-time PCR system (Applied Biosystems). The RT-qPCR analyses used two or three biological samples with two technical replicates each. Expression levels were calculated relative to the housekeeping gene *PeACTIN1* (Cutri & Dornelas, 2012) using the $2^{-\Delta\Delta Ct}$ method (Livak & Schmittgen, 2001). The primers used were designed to a unique sequence within the predicted coding region for each gene from sequences obtained by RNA-seq of *P. edulis* and *P. cincinnata* and are listed in Supplementary Table 1 (Table S1).

2.13 Analysis 5' Rapid amplification of cDNA ends (RACE)

Five micrograms of total RNA from leaves of *Passiflora edulis* was treat with DNase I (Invitrogen) and ligated to an RNA adapter following the manufacture's guide of GeneRacer kit (Invitrogen), the RNA ligation reaction was performed for 5 hours at 37 ºC. The complete amount of RNA was reverse transcribed to cDNA using the oligo dT from the GeneRacer kit and following the manufacture's guide of ImProm-II Reverse Transcriptase (Promega). The *PeSPL6* and *PeSPL13a* 5'-ends were amplified by PCR using the GoTaq Master mix (Promega), the forward 5' Primer from GeneRacer kit and the reverse Gene Specific Primer (GSP). The PCR product was used as a NESTED PCR template using the forward 5' Nested Primer from GeneRacer kit and the reverse Nested Gene Specific Primer (Nested GSP). The fragments size were confirmed by agarose gel (1%), the PCR fragments was purified using the Qiaquick PCR purification kit (Qiagen) and cloned into pGEM-T easy (Promega) vector. Nine independent clones from *PeSPL6* and two from *PeSPL13a* were sequenced using the forward M13 primer.

2.14 Sugar quantification

A pool of petiolar and laminar EFNs tissues isolated from fully expanded leaves was collected at midday. The samples were then macerated in liquid nitrogen and subjected to five successive treatment steps with 80% ethanol at 100°C for 5 min. After each extraction, the mixture was centrifuged (Eppendorf 5415D centrifuge) at 14000 rpm for 5 min. The total ethanolic extract obtained was evaporated at 50 °C and the sugars resuspended in 1 mL of 80% alcohol, subsequently the solution was filtered through an Econofilter membrane filter (Agilent technologies 0.2 μm). The filtrate was analyzed by high performance liquid chromatography (HPLC) (Shimadzu® series 20A, Kyoto, Japan), equipped with a column (Shim-pack GIST NH2 Shimadzu) and refractive index detector, containing the aminopropyl group (-NH2) as stationary phase. A mixture of acetonitrile and water (75:25) under isocratic conditions was used as a mobile phase. The analyses were performed at 40 °C, under flow rate of 1 mL/min. Sucrose, fructose and glucose were quantified using a calibration curve that correlates peak areas and known concentrations of the analyte.

2.15 Statistical analysis

Non-transgenic (NT) and miR156 overexpressing plants of *P. edulis* and *P. cincinnata* were placed in a greenhouse and completely randomized. Analysis of variance ($P < 0.05$) was used to determine the effect of treatments. The number and size of EFNs were evaluated using Tukey's test ($P \leq 0.05$), while other variables such as growth parameters, number of EFN tissue cells, gene expression, and quantification of sugars (sucrose, glucose, and fructose)were evaluated with Student's *t*-test ($P \leq 0.05$) in R-Bio® version 171 (hptts://biometria.ufv.br/; Bhering, 2017). Graphs were generated in Rstudio© v.1.4 using the ggplot2 package.

3 Results

3.1 High miR156 levels dramatically alters morphometric parameters and leaf morphology in *Passiflora* species

The age-dependent morphological changes observed in *P. edulis* leaves were associated with decreased miR156 expression and increased *PeSPL9* throughout phytomers (Silva et al., 2019). Similarly, in the early stages of *P. cincinnata* vegetative development, young leaves were trilobed and had elevated levels of miR156 (Fig. S1a). As the vegetative development progressed, leaves gradually became five-lobed and the levels of miR156 were strongly reduced and *PcSPL9* and miR172 transcripts increased (Fig. S1b-d). In *P. cincinnata* plants from seeds, EFNs do not develop until about the fourth leaf; interestingly, the developmental stage of leaves with lower and higher abundance of miR156 and *SPLs*, respectively, coincided with the presence of laminar EFNs in *P. edulis* (Silva et al., 2019, Fig. S1c) and *P. cincinnata* (Fig. S1).

To comprehensively investigate the conserved role(s) of miR156-targeted *SPLs* in leaf ontogeny and EFN formation in *Passiflora* species, we generated independent transgenic events overexpressing miR156 (hereafter referred to as miR156-OE or OE) in *P. edulis* (*Pe*OE) and *P. cincinnata* (*Pc*OE; Fig. S2a). The nuclear DNA content stability was maintained in all lines of miR156-OE compared with non-transgenic or control plants (NT: *Pe*NT and *Pc*NT) (Fig. S2b-d). *P. edulis* and *P. cincinnata* miR156-OE plants showed altered vegetative architecture (Fig. 1a) and exhibited a moderate bushy appearance. The miR156-OE plants in both species had reduced height and shorter 4th phytomer internode length than NT (Fig. 1b-c). Additionally, axillary buds thrived in the miR156-OE plants, contributing to the increasing branching index in *P. edulis* (~3-fold) and *P. cincinnata* (~1.5-fold) when compared with NT (Fig. 1d).

P. edulis plants derived from seeds exhibit monolobed leaves at the juvenile phase. As the vegetative phase transition progresses, leaves initiating at the 10th node become trilobed (Silva et al., 2019). *Pe*NT plants derived from *in vitro* showed the first trilobed leaf developed at the 6th node. In contrast, *Pe*OE plants produced monolobed, and slightly lobed leaves from 11 th to 12 th (Fig. 2a). In *P. cincinnata* plants derived from *in vitro* explants, the formation of the five-lobed leaf with completely individualized lobes occurred between the 6th to 7th nodes (Fig. 2b). On the other hand, *Pc*OE plants produced five-lobed leaves (7th to 8th nodes), but these leaves were less incised (margin deeply and sharply notched) than those in *Pc*NT plants. These results

indicated that the miR156/*SPL* module controls leaf heteroblasty in *Passiflora* species, similar to other species (Lawrence et al., 2021; Machado et al., 2023).

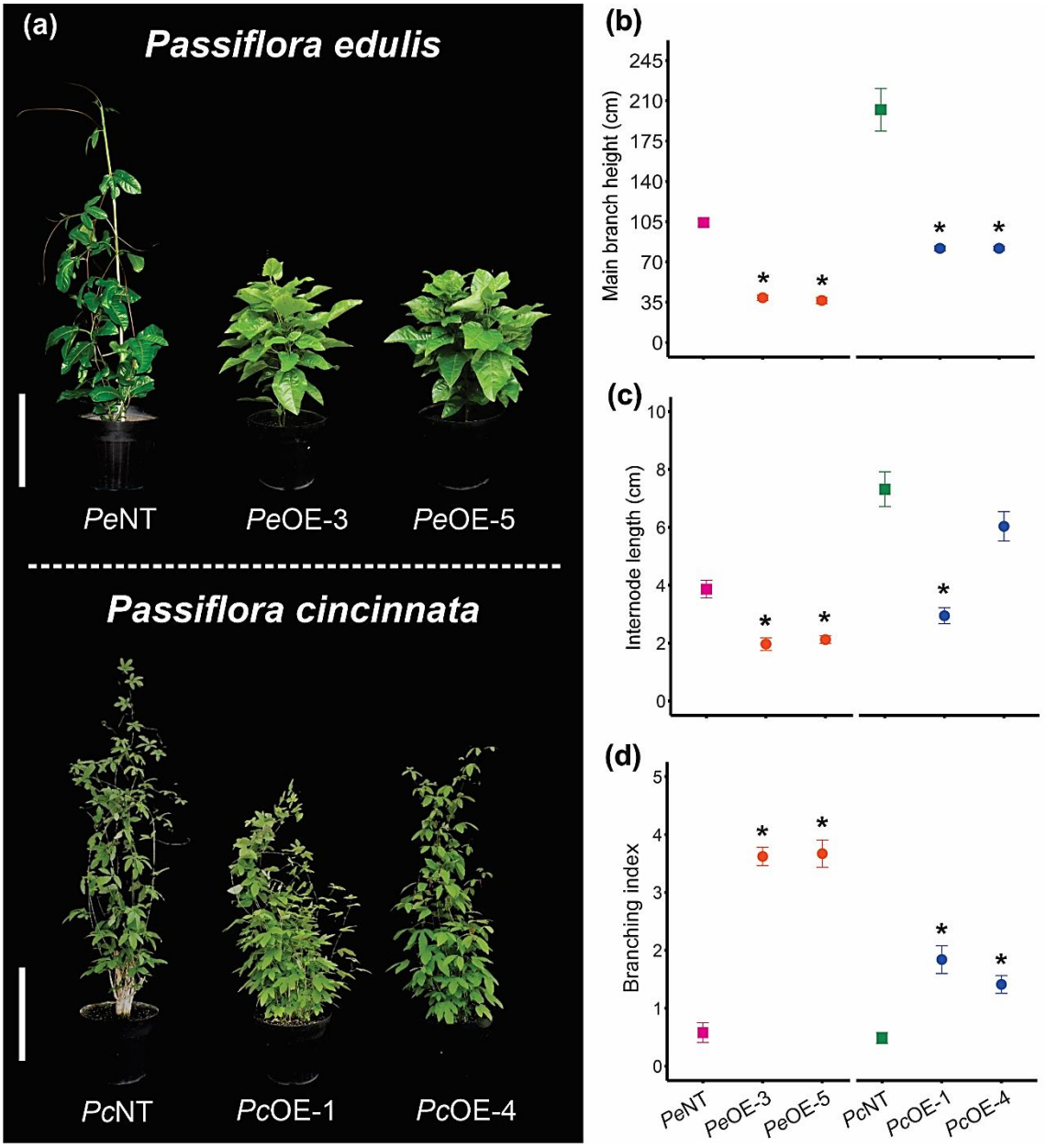

Figure 1: Shoot architecture is modified in miR156-overexpressing *Passiflora* species. (a) Vegetative architecture of non-transformed (*Pe*NT and *Pc*NT) and plants overexpressing miR156 (miR156-OE) in two distinct lines of *Passiflora edulis* (*Pe*OE-3 and *Pe*OE-5) on the 35th-day post acclimatization (DPA) and *Passiflora cincinnata* (*Pc*OE-1 and *Pc*OE-4) on the 60th DPA in a greenhouse. Scale Bar: 30 cm. (n=5). **(b)** Main stem height. **(c)** Internode length at 4 th node. **(d)** Branching index. Values are presented as mean ± SE (n=8). *$P \leq 0.05$ (Student's *t*-test).

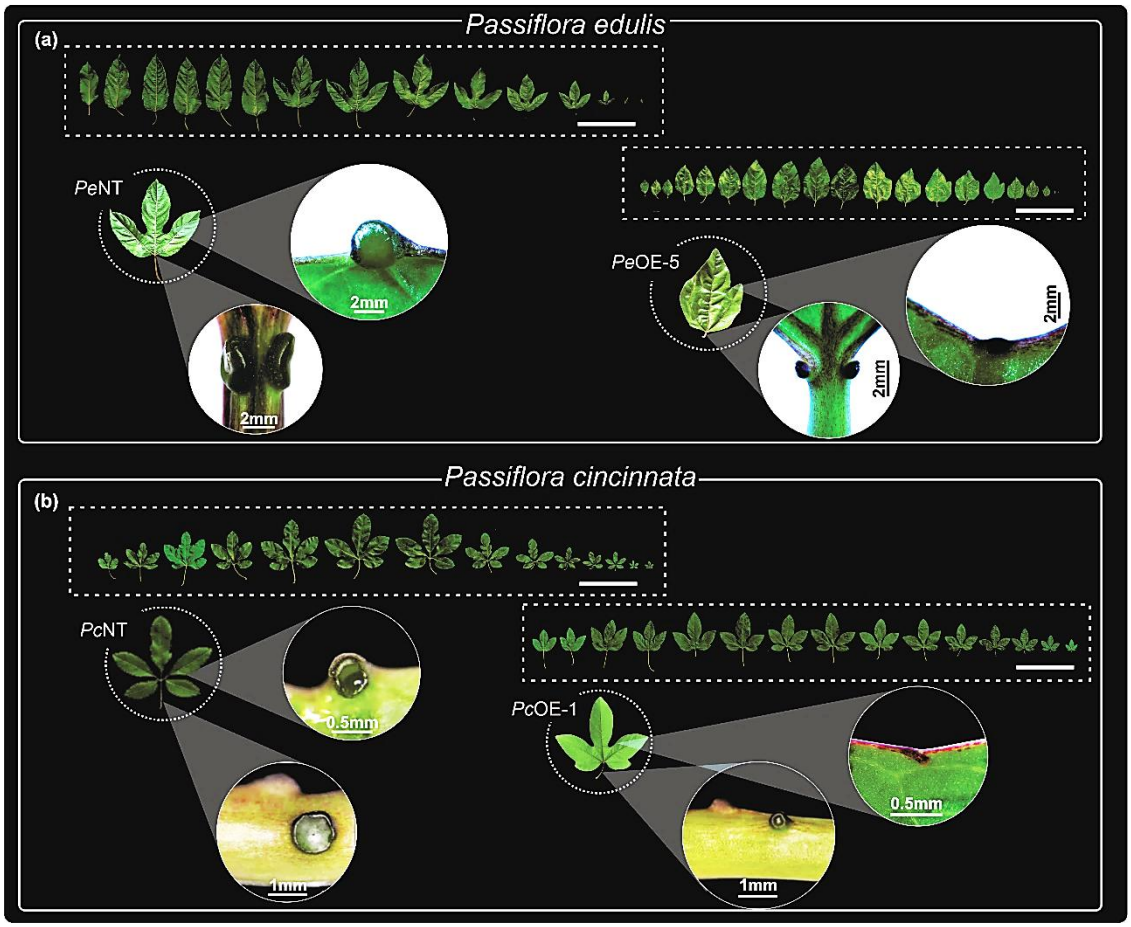

Figure 2: High levels of miR156 alter leaf heteroblastic development and extrafloral nectary (EFN) formation in *Passiflora* species. (a) Leaf morphology and EFN distribution in the petioles and leaf lamina of non-transformed (*Pe*NT) and over-expressing miR156 (*Pe*OE-5 plants of *Passiflora edulis* and **(b)** non-transformed (*Pc*NT) and over-expressing miR156 (*Pc*OE-1) plants of *Passiflora cincinnata*. Details of EFN of leaf 15 of *Pe*OE-5 line and leaf 12 of *Pc*OE-1. Scale Bar: 15 cm.

3.2 Extrafloral nectary size and abundance are age-dependent in *Passiflora* species

We examined whether additional aspects of leaf morphology—specifically the formation of EFNs—are regulated by the age-dependent miR156 pathway in *Passiflora* species. While *Passiflora* petiolar EFNs are paired and located on the adaxial site of the petiole, laminar EFNs are located abaxially on the leaf margin in the sinuses between leaf lobes (Fig. S1c; Fig. 2). For both species, EFNs of miR156-OE plants were underdeveloped or even absent in some cases when compared with NT plants (Fig. 2).

Reduced miR156 expression is correlated with the appearance of EFN in some *Vachellia* species (Leichty & Poethig, 2019). To examine the relationship between the age of the shoot and the formation of petiolar and laminar EFNs in *Passiflora* species, we performed a detailed analysis of these structures in different vegetative phases of NT (control) and miR156-OE plants. In the juvenile phase of *Passiflora edulis*, only petiolar EFNs are present in the monolobed leaves and remain during the adult phase in the trilobed ones. In contrast, laminar EFNs occur as the plant ages and its leaves develop lobes. In *Pe*NT plants showed a pair of petiolar EFNs on both the fourth (juvenile vegetative phase) and the 16th (adult vegetative phase) leaves and there was no difference in the diameter of these nectaries, but they did show a difference in the area (length x width) (Fig. 3a-c). *Pe*OE plants also had petiolar EFNs on nodes 4th and 16th, but they were smaller than *Pe*NT nectaries. *Pe*NT plants had 4 laminar EFNs on the 16th leaf (Fig. 3d), and PeOE plants had only one relatively small EFN (Fig. 3d-f).

In *P. cincinnata*, petiolar and laminar EFNs are found in both juvenile and adult vegetative stages. *Pc*NT plants had paired petiolar EFNs on the fourth (juvenile vegetative phase) and 12th (adult vegetative phase) leaves, but the nectaries were larger on the leaf 12 (Fig. 3g-i). *Pc*OE plants had fewer petiolar EFNs on leaf 4, but there was no difference in EFN number on leaf 12 compared with *Pc*NT (Fig. 3g). The size of the petiolar EFN on leaves 4 and 12 of *Pc*OE plants was 4- and 6-fold smaller than the nectaries of *Pc*NT plants, respectively (Fig. 3h-i). Both *Pc*NT and *Pc*OE leaves had an average of five laminar EFNs on leaf 4 (Fig. 3j), but they were smaller in diameter in *Pc*OE than *Pc*NT. There was no difference in the area of these nectaries, except for *Pc*OE-4, which had a smaller area (Fig. 3k-l). In contrast, *Pc*NT plants had an average of 18 larger laminar EFNs on leaf 12, whereas *Pc*OE plants had only 4-5 smaller EFNs (Fig 3j-l). In summary, the size was compromised in *P. edulis* miR156-overexpressing petiolar and laminar EFNs. On the other hand, both size and abundance of petiolar and laminar EFNs were negatively affected in *P. cincinnata* miR156-OE plants. Collectively, these observations indicated that the establishment and further development of EFNs are age-dependent in *Passiflora* species.

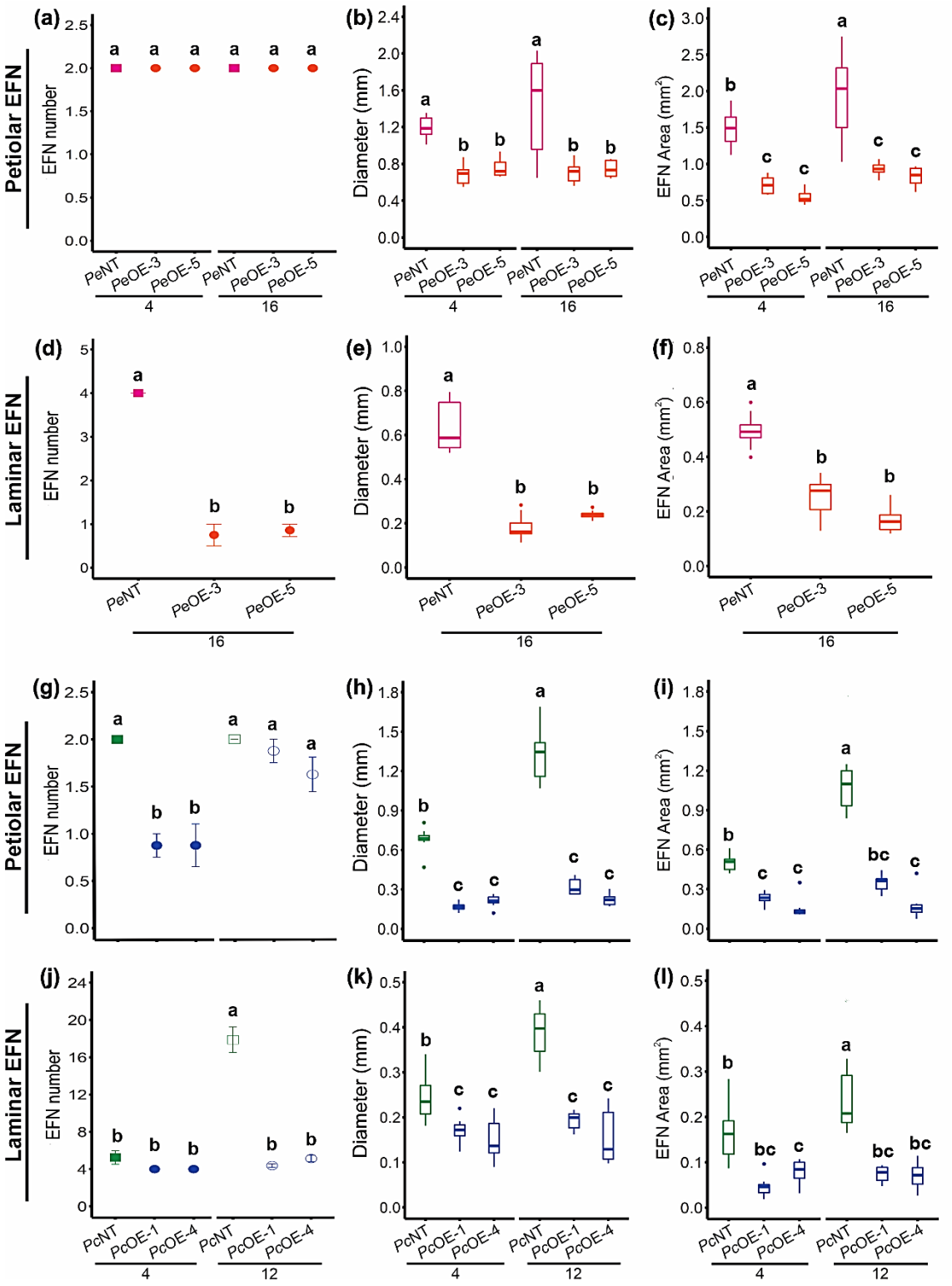

Figure 3: Extrafloral nectary (EFN) size and number are age-dependent in *Passiflora* species. (a) Number of petiolar EFN in non-transformed (*Pe*NT) and miR156-overexpression (*Pe*OE-3 and *Pe*OE-5) lines of *Passiflora edulis*. **(b-c)** Diameter and area (Length x Width) of petiolar EFN. **(d)** Number of laminar EFN in *Pe*NT, *Pe*OE-3, and *Pe*OE-5 plants. **(e-f)** Diameter and area of laminar EFN. **(g)**

Number of petiolar EFN in non-transformed (*Pc*NT) and *Passiflora cincinnata* miR156-overexpression (*Pc*OE-1 and *Pc*OE-4) lines. **(h-i)** Diameter and area of petiolar EFN. **(j)** Number of laminar EFN in *Pc*NT, *Pc*OE-1 and *Pe*OE-4 plants. **(k-l)** Diameter and area of laminar EFN. Numbers 4 and 16 in *P. edulis* and 4 and 12 in *P. cincinnata* correspond to leaf position (node). Values are presented as mean ± SE (n=8). *$P \leq 0.05$ (using ANOVA followed by Tukey's pairwise multiple comparisons).

To determine how miR156 affects EFN growth during early development, we next examined in more detail the morphoanatomy of EFNs from fully expanded adult leaves in NT and miR156-OE plants. In *Pe*NT, the laminar EFN has an elliptical shape with a concave central region (Fig. 4a; Lemos et al., 2017), whereas in *Pe*OE plants, the laminar EFNs developed as a protuberance with a convex surface (Fig. 4b-c). Although all three characteristic tissues (namely nectary epidermis, nectariferous parenchyma, and subnectariferous parenchyma) (Cardoso-Gustavson et al., 2013; Macêdo et al., 2021 Moraes et al., 2022) of the nectary were observed in *Pe*NT and *Pe*OE plants (Fig. 4d-f), the number of cells comprising each EFN tissue was reduced in *Pe*OE plants (Fig. 4m). In *P. cincinnata*, laminar EFNs have an obconical shape, curved towards the abaxial region of the leaves (Fig. 4g). In contrast, *Pc*OE-1 and *Pc*OE-4 showed an elongated cylindrical shape with an apex showing a convex surface or a small central cavity (Fig. 4h-i). Similar to *P. edulis*, tissue patterning was comparable between PcNT and PcOE (Fig. 4 j-l), but *Pc*OE laminar EFNs exhibited reduced cell number in each distinct tissue (Fig. 4n).

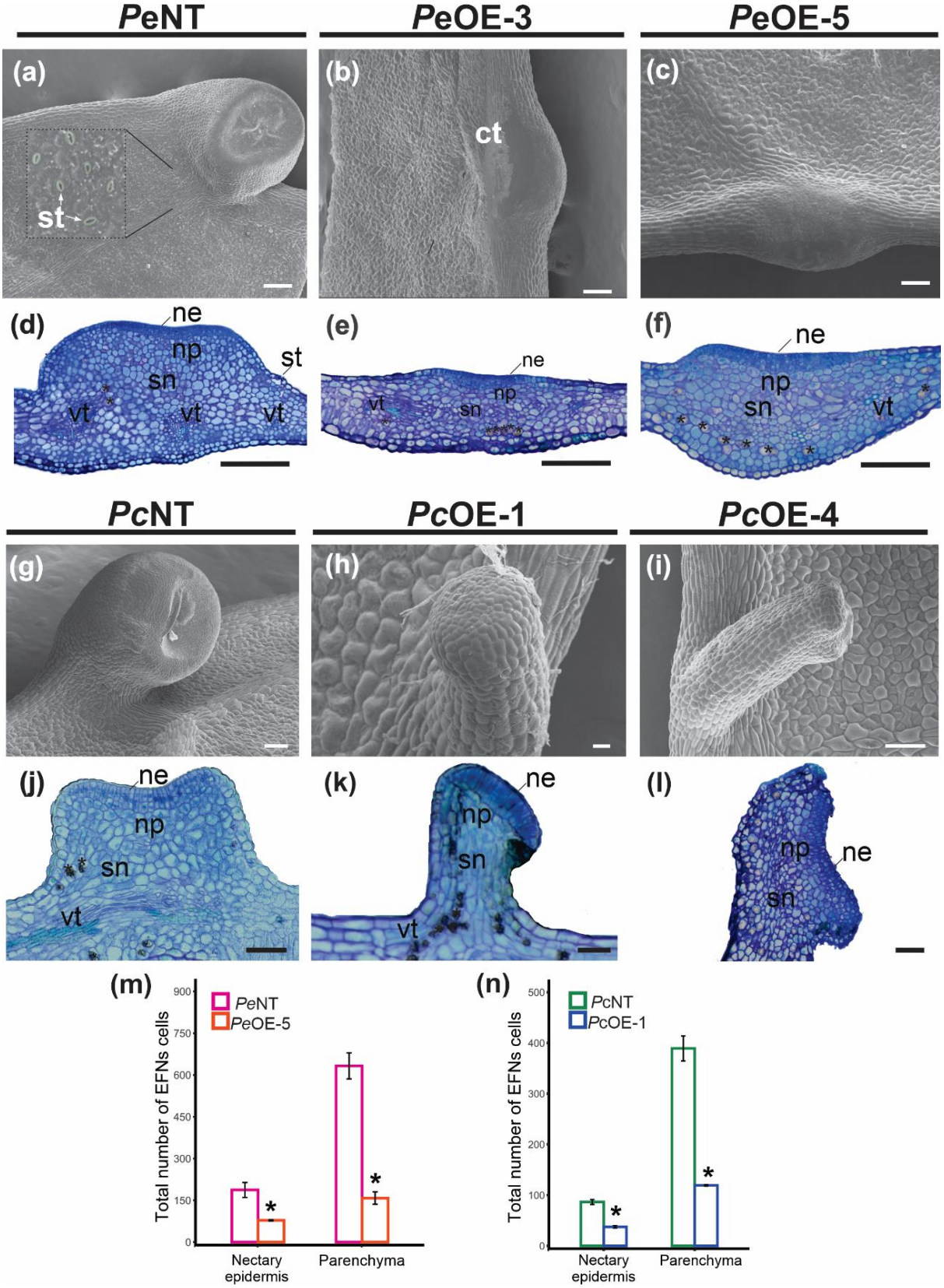

Figure 4: Cell number, but not patterning, of laminar extrafloral nectaries (EFN), is affected by high levels of miR156 in *Passiflora* leaves. Scanning electron microscopy images in *Passiflora edulis*: **(a)** Laminar EFN nectary in non-transgenic

(*Pe*NT) plants and **(b)** miR156-overexpression *Pe*OE-3 and **(c)** *Pe*OE-5 plants. Note the difference in morphology between non-transgenic and miR156-OE plants. ct: cuticle, st: stomata. Light microscopy in *P. edulis* plants: **(d)** Transverse section of the leaf showing a laminar EFN in *Pe*NT and **(e)** *Pe*OE-3 and **(f)** *Pe*OE-5 with three distinct regions: Nectary epidermis (ne), nectariferous parenchyma (np); subnectariferous parenchyma (sn); leaf vascular tissue (vt) and cells containing calcium oxalate crystals (*****). Scanning electron microscopy images in *P. cincinnata*: **(g)** Laminar EFN in non-transgenic (*Pc*NT) plant showing their secretory surface located at a concavity at medium-top region. **(h)** Laminar EFN showing an elongated shape in overexpressing miR156 plants *Pc*OE-1 and **(i)** *Pc*OE-4. Light microscopy **(j)** Transverse section of the leaf showing a laminar EFN in *Pc*NT and **(k)** *Pc*OE-1 and **(l)** *Pc*OE-4 plants showing the three distinct tissues. **(m)** Total number of cells of nectary epidermis and parenchyma (necteriferous + subnectariferous) of the laminar EFNs in *P. edulis* and **(n)** *P. cincinnata*. Values are presented as mean ± SE (n=3). **P* ≤ 0.05 (Student's *t*-test). Scale Bars: a-c = 100 μm, d-f = 50 μm, g=100 μm, h = 20 μm, i-l= 100 μm.

Petiolar EFN in *P. edulis* displays an elliptical shape with a small cavity in the center (Fig. 5a), through which nectar is released (Lemos et al., 2017). *P. edulis* miR156-OE plants showed petiolar EFNs with an elliptical shape similar to *Pe*NT, except for the cavity in the center of the nectary (Fig. 5b-c). Small elevations in the central region of the EFN were observed in *Pe*NT and *Pe*OE plants, probably representing nectar secretion that was retained in the subcuticular space (Fig.5 a-b). Petiolar EFNs in *Pc*NT plants also displayed an elliptical shape with a central concavity from which nectar is exuded (Fig. 5j). In *Pc*OE plants, on the other hand, petiolar EFNs exhibited a stipe-shape with a small central concavity (Fig. 5k-l). Similar to laminar EFNs, petiolar EFNs of NT and miR156-OE *Passiflora* plants are composed by nectary epidermis, nectariferous and subnectariferous parenchyma (Fig. 5d-i; m-s). Although NT and miR156-OE plants in *P. edulis* and *P. cincinnata* showed similar tissue patterning, the morphology and number of cells constituting the secretory tissue of petiolar and laminar EFNs were reduced in the miR156-OE plants, suggesting that cell division is compromised in miR156-overexpressing leaves.

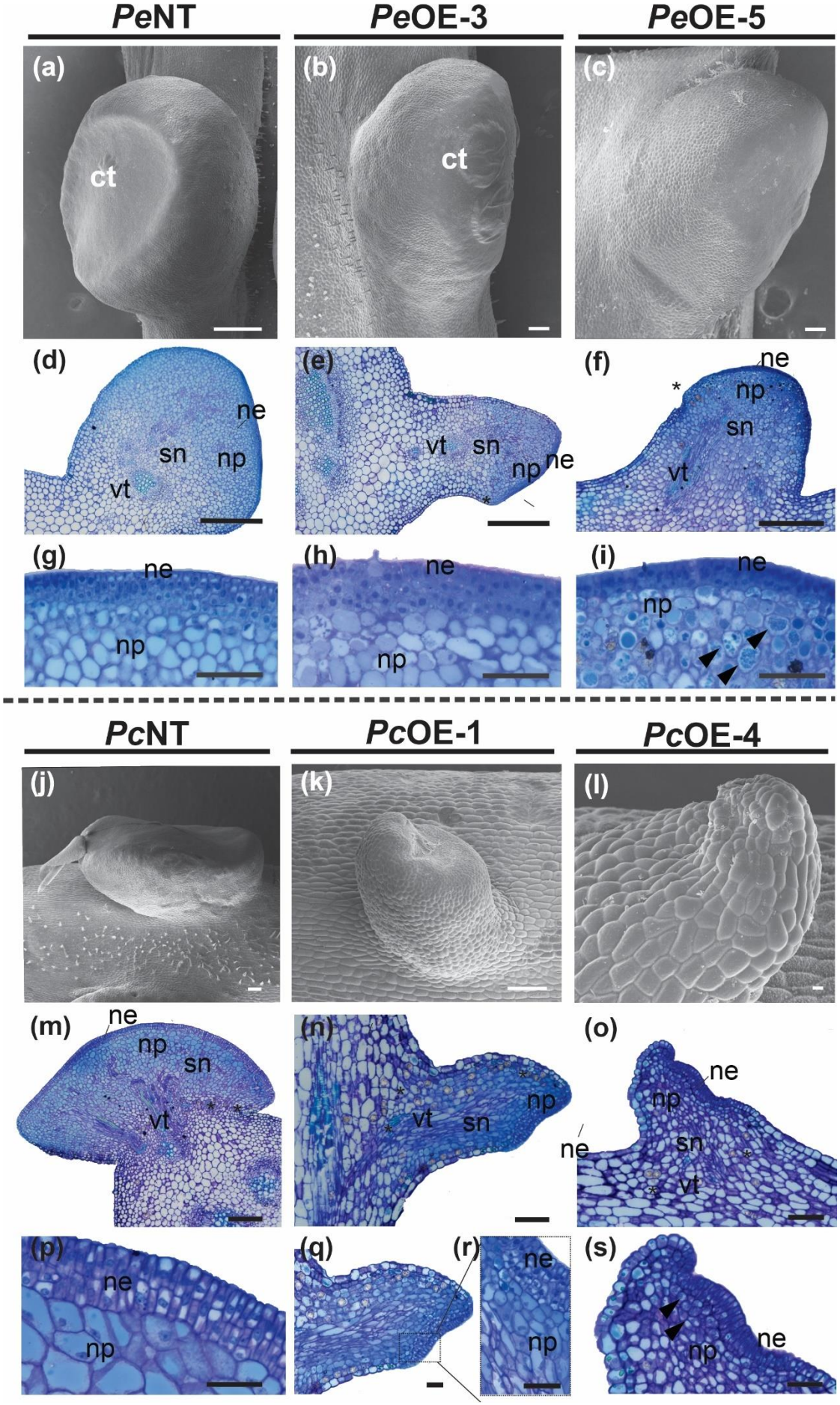
PeNT
PeOE-3
PeOE-5
(a)
(b)
(c)
ct
ct
(d)
(e)
(f)
ne
sn
np
vt
vt
sn
np
ne
ne
np
sn
vt
(g)
(h)
(i)
ne
np
ne
np
ne
np
PcNT
PcOE-1
PcOE-4
(j)
(k)
(l)
(m)
(n)
(o)
ne
np
sn
vt
vt
sn
np
ne
ne
np
sn
vt
(p)
(q)
(r)
(s)
ne
np
ne
np
ne
np

Figure 5: Morphology of *Passiflora* petiolar extrafloral nectaries (EFNs) is altered by the miR156 overexpression. Petiolar EFN Scanning electron microscopy (SEM) analysis in *Passiflora edulis* non-transgenic (*Pe*NT) **(a)**, *Pe*OE-3 **(b)** and *Pe*OE-5 **(c)** plants. Note the prominent cuticle with possible nectar content in the subcuticular region. Light microscopy *Passiflora edulis*: **(d, e)** Transverse sections of the leaf petiole showing petiolar EFN in *Pe*NT (**d**) and *Pe*OE-3 **(e). (f)** Longitudinal section in *Pe*OE-5 plants showing: Nectary epidermis (ne), nectariferous parenchyma (np); subnectariferous parenchyma (sn); leaf vascular tissue (vt) cells containing calcium oxalate crystals (*). (**g-i)** Detail of a petiolar EFN in *Pe*NT (**g**), *Pe*OE-3 **(h),** and *Pe*OE-5 **(i)**. **(j-l)** Petiolar EFN SEM in *P.cincinnata* in *Pc*NT**(j),** *Pc*OE-1 **(k),** and *Pc*OE-4 **(l)**. Note the ruptured cuticle in petiolar EFN *Pc*NT. **(m)** Transversal section of the petiole of leaf showing a petiolar EFN *Pc*NT. **(n,o)** Longitudinal sections of the *Pc*OE-1 **(n)** and *Pc*OE-4 **(o)** showing the three tissues of the nectary. **(p-r)** Detail of a petiolar EFN in *Pc*NT **(q)** and *Pc*OE-1 **(r)**, highlighting multiseriated epidermis. **(s)** Detail of a petiolar EFN in *Pc*OE-4, Arrowheads showing dense cellular content. Scale bar: a = 200 μm, b-c = 10 μm, d-f = 150 μm, g-i = 50 μm, j-k = 100 μm, l = 10 μm, m-o = 200 μm, p = 50 μm, q-s = 100 μm.

3.3 Transcriptional reprogramming of miR156-overexpressing *Passiflora* leaf primordia

To better understand the molecular mechanisms by which miR156 modulates leaf and EFN development, we employed RNA-seq to monitor changes in gene expression in *P. edulis* and *P. cincinnata* NT and miR156-OE leaf primordia, prior to the appearance of petiolar and laminar EFNs. After filtering low-quality reads, a total of 212,141 transcripts with average 677.33 bp and N50 equal to 1628 bp for *P. edulis* and 239,343 transcripts with average 629.10 bp and N50 equal to 1444 bp for *P. cincinnata* were assembled. Our functional annotation indicated that 58,087 ORFs (76.3%) and 63,376 ORFs (76.9%) were annotated in the SWISS-PROT database for *P. edulis* and *P. cincinnata*, respectively. The RNA-seq analysis detected 1048 differentially expressed genes (DEGs) in *P. edulis* (FDR > 0.05 and fold change >1.5), including 407 up-regulated and 641 down-regulated genes (Fig. S3a; Table S2). In *P. cincinnata*, a total of 667 DEGs were identified, including 316 up-regulated and 351 down-regulated genes (Fig. S3b; Table S3). Gene Ontology (GO) analysis classified DEGs (P < 0.05) into three categories, biological process, cellular component and molecular function (Fig.

S4). In general, DEGs were more enriched in the biological process category, which included genes associated with regulation of vegetative phase change (GO: 0010321), development of the shoot reproductive system (GO: 0090567), flower development (GO: 0009908), and senescence of floral organs (GO: 0080187).

To characterize the effects of constitutive miR156 expression on *SPL* transcript levels we first interrogated our RNA-seq data to identify *SPL* sequences using TransDecoder (https://github.com/TransDecoder/TransDecoder). This revealed a set of eight *P. cincinnata* and nine *P. edulis SPL* members, referred to as *PcSPLs* and *PeSPLs* respectively, detected across our samples (Fig. 6a). Phylogenetic analyses demonstrated that these genes represented all the major clades of *SPL* family members previously described. *PeSPL/PcSPL* genes were annotated based on the closest phylogenetic relationship with *Arabidopsis* and grape *SPLs* (Salinas et al., 2012; Preston & Hileman, 2013; Table S4). Five *SPLs* (*PcSPL6*/*PeSPL6*, *PcSPL9*, *PcSPL13a*/*PeSPL13a*, *PcSPL13b*/*PeSPL13b*, *PeSPL13s*) contain the target site for miR156 in their transcript sequences (Fig. 6b).

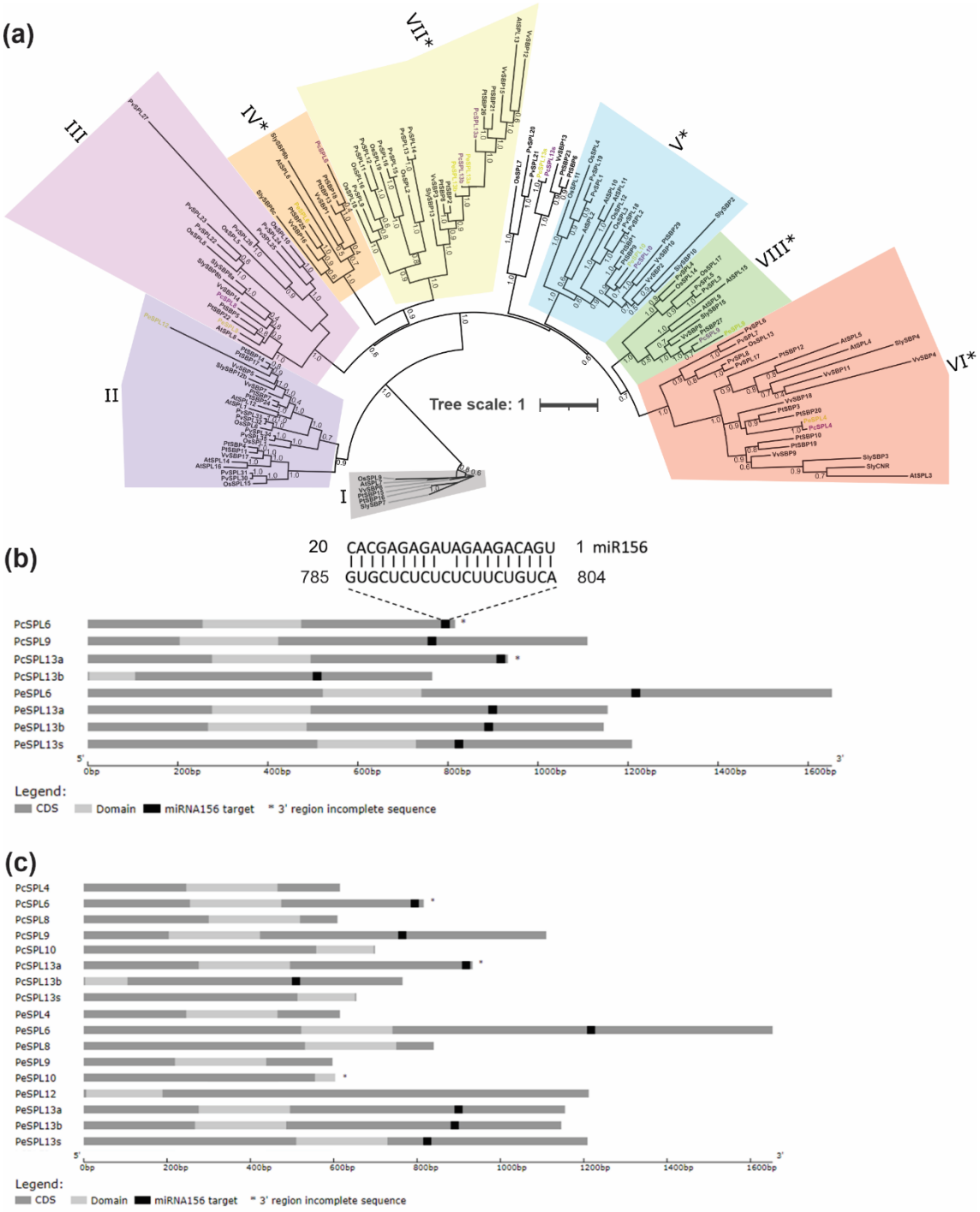

Figure 6: Maximum-likelihood phylogeny of the miR156-targeted *SPL*/SBP proteins of *Passiflora* species. (a) Unrooted phylogenetic tree based on an alignment of all *SPL*/SBP sequence encoded protein obtained for *P. cincinnata* (*PcSPL*), *P. edulis* (*PeSPL*), tomato (*SlySBP*), Arabidopsis (*AtSPL*), poplar (*PtSBP*), grapes (*VvSBP*), rice (*OsSPL*), and swithgrass (*PvSPL*), using MUSCLE tool and Interactive Tree of Life (iTOL) resource to annotate. Original code gene for each species is available (Table

S4). Clade colors match Salinas et al. (2012) where applicable. Clade with asterisks is regulated by miR156 or miR157, as stated by Preston and Hileman (2013). The code names of *P. edulis* and *P. cincinnata SPLs* were marked in yellow and purple, respectively, for highlight; those with asterisks contain predictable target region for miR156 in their sequence (Table S5). Scale bars indicate the number of substitutions per site. **(b)** Heavy grey lines represent ORFs. The light grey box represents SBP domain. miRNA complementary sites (black box) with the nucleotide positions of *Passiflora SPLs* sequences are indicated. Asterisk means incomplete 3`region from a detected transcript. **(c)** *Passiflora SPLs* non-targeted and targeted by miR156. Heavy grey lines represent ORFs. The light grey box represents SBP domain. miRNA complementary sites (black box) with the nucleotide positions of *Passiflora SPLs* sequences are indicated. Asterisks mean incomplete 3` sequences.

Among the identified miR156-targeted *SPLs*, *SPL4*, *SPL6*, *-9*, and *-13a* were strongly repressed in miR156-OE lines relative to NT plants in both species (Fig. 7a-g), suggesting they are strong candidate regulators of heteroblastic leaf development in *Passiflora*. To determine whether miR156 regulates any non-*SPL* targets we employed psRNATarget (Dai et al., 2018). Similar to other species we found no well-supported targets outside of the *SPL* family (Table S5). To confirm that miR156 directly targets *Passiflora SPL* transcripts we identified miR156 cleavage sites in *PeSPL6* and *PeSPL13a* by 5' RACE (Fig. 7h). This would suggest that, similar to *Arabidopsis* (He et al., 2018), miR156 functions at least in part through transcriptional cleavage in *Passiflora*.

Overexpression of miR156 and the consequent reduction in *SPL* activity in *Passiflora* impacted the expression of several genes associated with leaf ontogeny, such as *YABBY1* (*YAB1*) and *YAB5*. Members of the *YABBY* gene family, including the floral nectary-enriched *YAB5* and CRABS *CLAW* (*CRC*), are expressed abaxially in leaves and floral organs and are responsible for establishing or interpreting organ polarity in *Arabidopsis* (Siegfried et al., 1999; Bowman & Smyth, 1999; Eshed et al., 1999). We detected transcripts of *YAB1* and *YAB5* that were downregulated in miR156-OE leaf primordia in both species (Fig. 7 a, b, i, j; Table S2, S3). On the other hand, *ASYMMETRIC LEAVES1* (*AS1*), which regulates dorsoventral polarity (Husbands et al., 2015), and orthologs of *AUXIN TRANSPORTER-LIKE PROTEIN 2* (*LAX2*), which regulates leaf margin serration in *Arabidopsis* (Kasprzewska et al., 2015), were

upregulated in *Passiflora* miR156-OE lines (Fig. 7a , k, l; Table S3). Interestingly, the *SUCROSE TRANSPORT PROTEIN 2* (*SUC2*) gene, responsible for sucrose transport (Chandran et al., 2003), was downregulated in miR156-OE plants (Fig. 7m). *Passiflora AGAMOUS-like MADS-box 14* (*AGL14*), *AGL19* and *AGL104* were all downregulated in miR156-OE leaf primordia (Fig. 7a, b, n), which suggests that *SPLs* may be required for their activation. Other genes necessary for floral nectary development (Chen et al., 2021), such as *LEAFY*, were also downregulated in *PeOE* leaf primordia (Table S2). Collectively, our data are consistent with the hypothesis that the miR156/*SPL* module has been coopted into the regulation of genetic networks associated with nectary development.

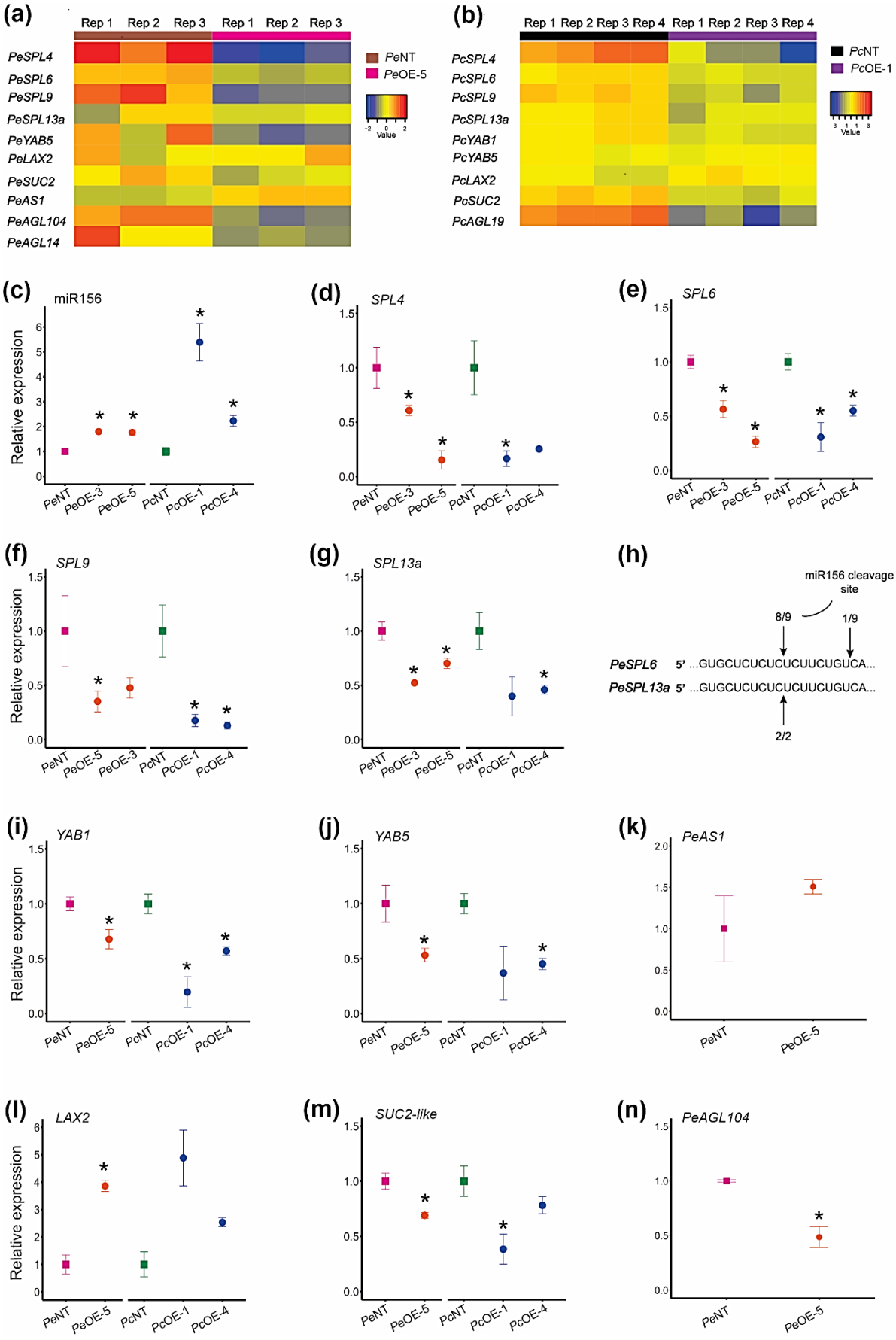
(a)
Rep 1 Rep 2 Rep 3 Rep 1 Rep 2 Rep 3
PeSPL4
PeSPL6
PeSPL9
PeSPL13a
PeYAB5
PeLAX2
PeSUC2
PeAS1
PeAGL104
PeAGL14
PeNT
PeOE-5
Value
(b)
Rep 1 Rep 2 Rep 3 Rep 4 Rep 1 Rep 2 Rep 3 Rep 4
PcSPL4
PcSPL6
PcSPL9
PcSPL13a
PcYAB1
PcYAB5
PcLAX2
PcSUC2
PcAGL19
PcNT
PcOE-1
Value
(c)
miR156
Relative expression
PeNT
PeOE-3
PeOE-5
PcNT
PcOE-1
PcOE-4
(d)
SPL4
(e)
SPL6
(f)
SPL9
(g)
SPL13a
(h)
miR156 cleavage site
8/9
1/9
PeSPL6 5' ...GUGCUCUCUCUCUUCUGUCA...
PeSPL13a 5' ...GUGCUCUCUCUCUUCUGUCA...
2/2
(i)
YAB1
(j)
YAB5
(k)
PeAS1
(l)
LAX2
(m)
SUC2-like
(n)
PeAGL104

Figure 7: miR156 overexpression affects levels of *SPLs* and genes associated with leaf ontogeny and nectary development in *Passiflora*.

Identification of differentially expressed genes (DEGs) up-regulated (red) and down-regulated (blue) by RNA-seq analysis in leaf primordia of non-transgenic (NT) plants compared with overexpressing miR156 (miRNA-OE) plants in **(a)** *Passiflora edulis* and **(b)** *P. cincinnata*. R1 to R4 indicate biological replicates. **(c)** Relative expression by RT-qPCR analysis of miR156 in *P. edulis* (*Pe*NT, *Pe*OE-3, *Pe*OE-5) and *P. cincinnata* (*Pc*NT, *Pc*OE-1, *Pc*OE-4), **(d)** *SPL4,* **(e)** *SPL6,* **(f)** *SPL9*,**(g)** *SPL13a,* **(h)** Modified 5'-RACE analyzes of cleaved *PeSPL6* and Pe*SPL*13a transcripts in Passiflora edulis leaf tissue. The 5'-ends of *PeSPL6* and *PeSPL13a* map to miR156 recognition site. **(i)** Relative expression of *YAB1*, **(j)** *YAB5* , **(k)** *AS1* in *P. edulis*, **(l)** *LAX2*, **(m)** *SUC2-like*, **(n)** *AGL104* in *P. edulis*. Values are presented as means ± SE (n=3). $*P \leq 0.05$ (Student's *t*-test).

3.4 Ecological relationships and sugar profile of extrafloral nectaries are affected in miR156-overexpressing *Passiflora*

Passiflora EFNs offer nectar to territorial and aggressive ants, establishing important mutualistic and ecologically impactful relationships (Cardoso-Gustavson et al., 2013). To determine whether *SPL* activity is important for the function of EFNs we evaluated ant visitation of both *P. edulis* and *P. cincinnata* plants in the greenhouse for 10 days at the period of highest ant activity. Visiting ants belong to the genus *Brachymyrmex*, which are ~3mm in lenght with an acidopore and 9-segmented antennae that lacks an antennal club (Fig. 8a; Ortiz-Sepulveda et al., 2019). Ant visitation was significantly reduced in *P. edulis* and *P. cincinnata* miR156-OE plants compared to *Pe*NT and *Pc*NT (Fig. 8b-c).

The nectar exuded by EFNs is rich in carbohydrates and is an attractant for food-seeking ants (Cardoso-Gustavson et al., 2013). EFNs in miR156-OE plants are smaller than in NT plants (Fig. 3), which might make them less attractive to ants. In addition, the quality of the nectar is impacted by the size of EFNs in different species, and affects ant visitation (Alencar et al., 2023). We therefore evaluated nectar availability and carbohydrate content in the EFNs from miR156-OE and NT plants. Although nectar availability was consistently observed in miR156-OE plants in both species during the evaluated period, the sucrose content of *Pc*OE EFNs was significantly lower than *Pc*NT (Fig. 8d). On the other hand, fructose content was higher

in *Pc*OE and glucose level was comparable with *Pc*NT nectaries (Fig. 8 e-f). In *P. edulis* EFNs, sucrose was not detected, and fructose and glucose content showed no significant differences between *Pe*OE and *Pe*NT, although *Pe*OE nectaries showed slightly higher fructose and lower glucose content compared to *Pe*NT (Fig. S5a-b). Collectively, our results indicate that low abundance and defective EFN patterning combined with modifications in carbohydrate composition of the nectar correlate with the reduced ant visitation observed in miR156-OE *Passiflora* plants. Thus, age-dependent miR156-targeted *SPLs* might be required for the ecological interaction potential of *Passiflora* species.

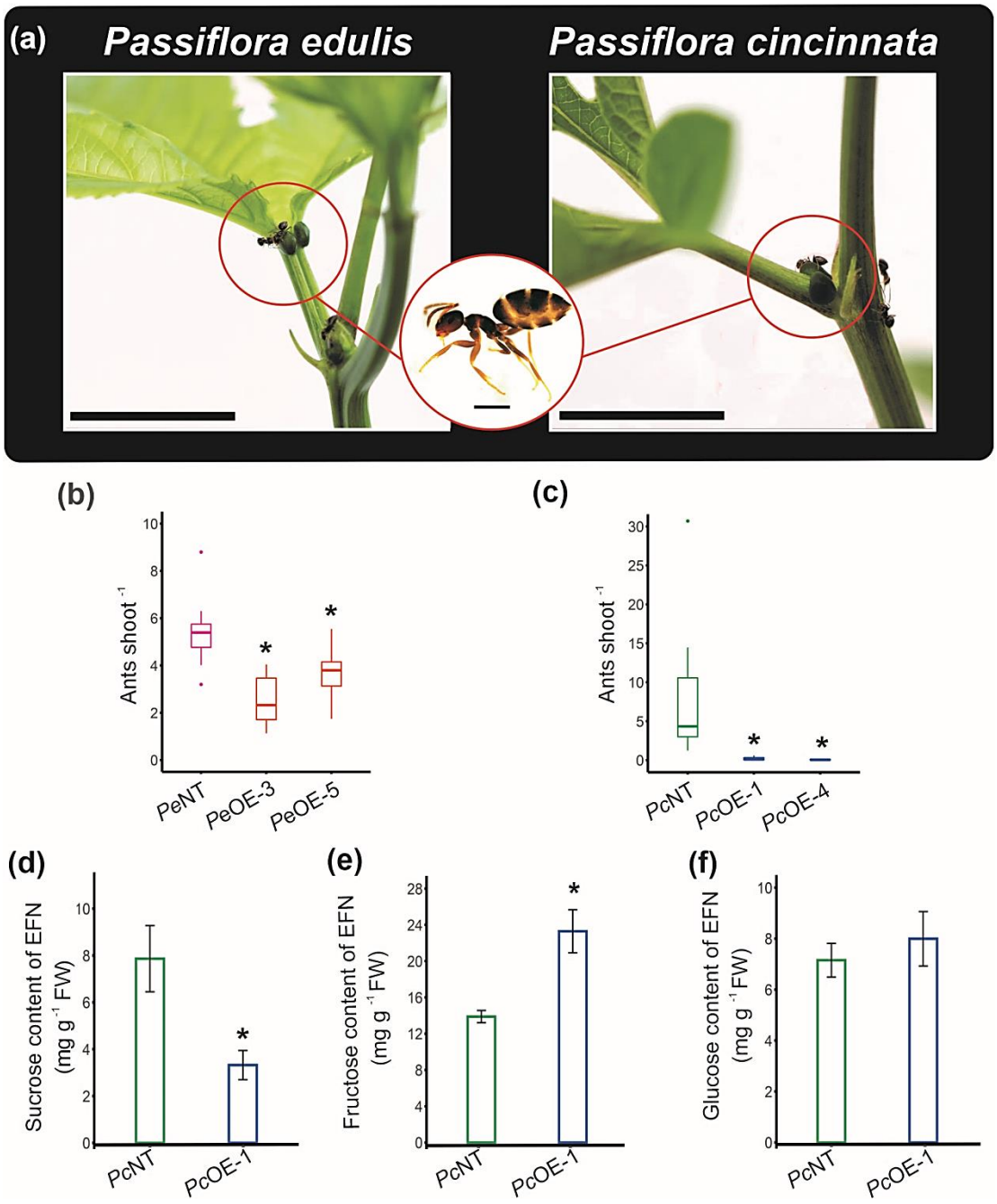

Figure 8: Reduced *SPL* expression modified sugar profiles in miR156-overexpressing *Passiflora* extrafloral nectaries (EFNs), and negatively impacted ant visitation. (a) Ants collecting nectar on petiolar EFNs of *Passiflora edulis* and *P. cincinnata*. Scale Bar:1cm. Detail of the ant *Brachymyrmex* spp. Scale Bar: 0.5 mm. **(b, c)** Ant visitation values per plant are presented as mean ± SE in non-transgenic (NT) and *P. edulis* overexpressing miR156 (*Pe*OE-3 and *Pe*OE-5**)** and **(b)** *P. cincinnata* (*Pc*OE-1 and *Pc*OE-4**) (c)** (n= 8-9). **(d)** Sucrose, **(e)** fructose, and **(f)** glucose content of the laminar and petiolar EFN pool of *Pc*NT and *Pc*OE-1 (n = 3). *$P \leq$ 0.05 (Student's *t*-test).

4. Discussion

Temporal patterning of shoot development in *Passiflora* species likely requires the activity of miR156-targeted *SPLs*

Leaf heteroblasty is used as a taxonomic trait for several *Passiflora* species, and can distinguish between juvenile and adult phases of vegetative growth (Chitwood & Otoni 2017 a, b; Silva et al., 2019). Similar to *P. edulis* (Silva et al., 2019), vegetative maturation in *P. cincinnata* is also associated with pronounced changes in leaf morphology that occur gradually in successive phytomers and correlate negatively and positively with changes in miR156 and *SPL* transcript levels, respectively (Fig. S1). In *Arabidopsis*, *SPL*-dependent heteroblastic changes in leaf morphology are determined by altered rates of growth of different domains of the leaf and phase-specific patterns on cell division and expansion (Hu et al., 2023; Tang et al., 2023; Li et al., 2024). Whether similar mechanisms regulate progressively increased leaf lobing in *Passiflora* will be a key future area of research.

Constitutive expression of miR156 maintained *Passiflora* plants in the juvenile phase, supporting the conservation of miR156 function across the angiosperms. However, a slight increase in leaf lobing was observed over time even in *PeOE* and *PcOE* plants (Fig. 2). This may reflect increased *SPL* transcription, as miR156 has been shown to regulate *SPL* activity in a dose-dependent manner (Fu et al., 2012; He et al., 2018). Conversely, it may reflect miR156-independent mechanisms of shoot maturation (He et al., 2018; Fouracre et al., 2021). Unlike the NT controls, neither *Pe*OE nor *Pc*OE plants flowered during the course of our experiments. This would suggest that *SPL* activity is critical for floral induction in *Passiflora*, at least in our growth conditions. Although miR156 does not play a major role in flowering time in *Arabidopsis* (Doody et al., 2022; Zhao et al., 2023; Poethig & Fouracre, 2024), *SPL* activity is an important determinant of flowering time in other species, including tobacco, alfalfa and switchgrass (Feng et al., 2016; Aung et al., 2015; Johnson et al., 2017).

EFN formation is regulated in an age-dependent manner in *Passiflora*

Phase-specific traits, such as the presence of EFNs, have been previously identified during vegetative phase change in woody species (Leichty & Poethig, 2019; Machado et al., 2023). We showed here that the formation of EFNs is age-dependent in

two *Passiflora* species and associated with heteroblastic changes to leaf morphology. During the juvenile vegetative phase, *P. edulis* produces simple leaves with petiolar EFNs, which are present consistently throughout vegetative development. During the transition from the juvenile to the adult vegetative phase, leaf morphology gradually changes and becomes tri-lobed (Silva et al., 2019), simultaneously forming nectaries on the inner side of the leaf margin furrow. EFNs are already present in the tri-lobed juvenile leaves of *P. cincinnata*; however, the increase in the number of leaf lobes leads to an increase in the abundance of nectaries at the margin (Fig. S1), which was inhibited by high levels of miR156 (Figs. 2, 3). This observation indicates that *P. cincinnata* EFN formation/abundance in the leaf margin partially depends on the miR156/*SPL* module. Importantly, laminar EFN development and lobe formation increase concurrently, suggesting that these two leaf development aspects are regulated by an age-dependent pathway. Interestingly, a similar phenomenon is observed in leguminous *Vachellia* species, in which age-dependent production of EFNs evolved independently (Leicthy & Poethig, 2019). This would suggest that the miR156/*SPL* module has been coopted repeatedly during angiosperm evolution to regulate the timing of EFN production.

The size and abundance of laminar EFNs are greater in the adult phase, concomitant with an increase in leaf complexity and *SPL* transcript levels. In *Passiflora* miR156-OE lines, the size of the leaf lamina, as well as the size of petiolar and laminar EFNs was reduced (Fig. 3), suggesting that the ontogeny of these structures was affected by low *SPL* expression and that changes in leaf development affect the growth of EFNs. Although the morphology of EFNs was affected in miR156-OE *Passiflora* plants, their tissue patterning was similar to NT plants, with demarcated nectary epidermis and nectariferous and subnectariferous parenchyma (Lemos et al., 2017; Moraes et al., 2022). However, cell number was strongly reduced mostly in the parenchymatic tissues (Fig. 4m, n). These findings suggest that *SPL* genes regulate overall growth of EFNs, rather than specifying EFN cell identity. The effect of *SPL* proteins on rates of cell division is consistent with recent findings in *Arabidopsis* and tomato (Tang et al., 2023; Ferigolo et al., 2023; Li et al., 2024).

miR156 regulates genes associated with *Passiflora* leaf patterning and EFN development

In addition to regulating leaf identity, the miR156/*SPL* module may also regulate EFN-associated genes. By analyzing the transcriptome data from *Passiflora*

leaf primordia prior to EFN formation, we propose that miR156-targeted *SPLs* may regulate early EFN formation at the molecular level (Table 2, 3; Fig. 6, 7). Reduced *SPL* expression in miR156-OE leaf primordia led to the misexpression of genes associated with *Passiflora* leaf and EFN development, suggesting that these genes act together with the miR156/*SPL* module in a complex network (Nakayama et al., 2022).

For instance, *AS1* transcript levels were slightly increased in miR156-OE plants (Fig. 7; Tables S2, S3). Given that *AS1* is a member of the ARP family (*AS1*/ *RS2*/ *PHAN*) involved in adaxial identity and leaf complexity (Husbands et al., 2015; Nakayama et al., 2022), higher levels of *AS1* in miR156-OE may have affected the adaxial-abaxial patterning of leaf primordia, which is fundamental for proper EFN establishment.

Adaxial-abaxial polarity is also regulated by *YAB1* and *YAB5*. Importantly, *YAB5* is associated with the heteroblastic leaf development and floral nectary formation (Kram et al., 2009; Ostria-Gallardo et al., 2016; Chen et al., 2021). Thus, the presence of stunted EFNs in *Passiflora* miR156-OE leaves (Fig. 2) may be partially due to the low expression levels of *YAB1* and *YAB5* in the leaf primordia (Fig. 7; Table S2, S3). High levels of *LAX2-like* (Fig. 3; Table S2, S3), an auxin importer strongly associated with *Arabidopsis* leaf margin serration (Kasprzewska et al., 2015), might have led to impaired lobe formation in *Passiflora* miR156-OE leaf margins. Interestingly, tomato miR156-targeted *SPL15* negatively regulates auxin transport in the axillary buds partially via *LAX2* (Barrera-Rojas et al., 2023). Transcript levels of several *MADS-box* genes were lower in miR156-OE (Fig. 7; Table S2, S3), suggesting that the activation of these genes may depend on *SPL* expression. *AGAMOUS-like MADS-box* genes (*AGLs*) are direct targets of miR156-directed *SPLs* in *Arabidopsis* (Wang et al., 2009; Gao et al., 2018), and are involved in promoting leaf complexity and floral nectary development (Kram et al., 2009; Ostria-Gallardo et al., 2016; Chen et al., 2021). The use of distinct *Arabidopsis* floral homeotic mutants demonstrated that proper floral nectary development requires *AG* and *AGL* genes (Slavković et al., 2021).

The changes in the morphology and sugar profile of miR156-OE EFNs affect *Passiflora* ecological relationships

EFNs promote mutualistic interactions with ants that act as defenders against herbivores in exchange for nectar, thereby establishing an indirect defense mechanism

(Elias, 1983; Apple & Feener, 2001; Heil, 2015). Interestingly, EFNs increase in number in both *P. edulis* and *P. cincinnata* as the plant ages, suggesting that ant recruitment is prioritized during the adult phase. Although miR156-OE EFNs differentiate all the tissues necessary for nectar production and exudation, ant visitation was lower in miR156-OE lines of both *Passiflora* species. Changes in nectary size and abundance may partially explain the behavior of ants towards miR156-OE plants. Species with abundant, more prominent and accessible EFNs attract more ants than those with smaller nectaries, increasing defense performance (Apple & Feener, 2001; Alencar et al., 2023). Removing EFNs reduces ant patrolling, but mechanically damaging EFNs without affecting nectar supply has not been shown to limit ant visitation (Izarigue et al., 2013). Other variables, such as nectar quality and quantity, interfere with plant-animal mutualistic interactions (Heil, 2011; Alencar et al., 2023). The altered sugar profile in miR156-OE EFNs may have contributed to the observed reduction in ant patrolling (Fig. 8). It is important to note that the lower sucrose content might be associated with lower expression of *SUC2-like* transporters in miR156-OE leaf primordia (Fig. 7; Table S2, S3), as during the nectar secretion phase of wild type EFNs, genes encoding sucrose transporter are up-regulated (Chatt et al., 2021). Nectar with high concentrations of sugars seems to be more attractive to ants than those with low concentrations, resulting in increased visitation and persistence of the protective agent on the plant (Villamil et al., 2013; Alencar et al., 2023).

The nectar of EFNs in *Passiflora* species is chemically diverse and may contain alkaloids and flavonoids, and its consumption may depend on the metabolic capacity or preference of the consumer (Heil et al., 2011; Cardoso-Gustavson et al., 2013). Therefore, we cannot exclude the possibility of changes in the content of other chemical compounds present in the nectar of *Passiflora* miR156-OE EFNs may lead to a reduction in ant visitation. Because EFN visitors are defined as opportunistic species and do not always provide defensive assistance, it was not possible at this point to establish a specific mutualist relationship between the evaluated ants and *Passiflora* species. In addition, arthropod-plant interactions mediated by EFNs can be rapidly established between species that do not have a co-evolutionary relationship (Heil et al., 2015).

In summary, our observations indicate that the miR156-targeted *SPL* function may be fundamental for the establishment of EFNs in two *Passiflora* species with

distinct leaf shapes. Further studies of molecular mechanisms that trigger extrafloral nectary establishment and patterning may provide valuable information for *Passiflora* yield improvement, as EFNs are key structures involved in strategies against herbivory in the genus *Passiflora*.

5. Conclusions

The results presented here provide the first evidence for the involvement of the miR156/*SPL* pathway in the regulation of EFNS development in *Passiflora* species. Based on our results, we conclude that:

- Low levels of miR156-targeted *SPLs* in miR156-overexpressing *P. edulis* and *P. cincinnata* plants prolonged the juvenile phase and affected heteroblastic leaf patterning.
- Anatomical, transcriptome, and sugar content analyses revealed that miR156-targeted *SPLs* are required for proper *Passiflora* laminar EFN ontogeny and mutualistic interaction with ants.
- The development of EFNs can be modulated by a preexisting genetic program in the organ bearing them, and that the formation and abundance of laminar EFNs in *Passiflora* species is correlated with the formation of lobes during the age-dependent heteroblastic leaf development.

6. References

Alencar CLDS, Nogueira A, Vicente R E, Coutinho IAC. 2023. Plant species with larger extrafloral nectaries produce better quality nectar when needed and interact with the best ant partners. *Journal of Experimental Botany* **74 (15):**4613–4627.

Anisimova M, Gascuel O. 2006. Approximate likelihood-ratio test for branches: A fast, accurate, and powerful alternative. *Systematic Biology* **55(4):** 539–552

Apple, JL, Feener DH. 2001. Ant visitation of extrafloral nectaries of *Passiflora*: The effects of nectary attributes and ant behavior on patterns in facultative ant-plant mutualisms. *Oecologia* **127**: 409–416

Aung B, Gruber MY, Amyot L, Omari K, Bertrand A, Hannoufa A. 2015. Ectopic expression of *LjmiR156* delays flowering, enhances shoot branching, and improves forage quality in alfalfa. *Plant Biotechnology Reports* **9**: 379-393.

Arshad M, Feyissa BA, Amyot L, Aung B, Hannoufa A. 2017. MicroRNA156 improves drought stress tolerance in alfalfa (*Medicago sativa*) by silencing *SPL*13. *Plant Science* **258**: 122–136.

Barrera-Rojas CH, Vicente MH, Brito DAP, Silva EM, Lopez AM, Ferigolo LF, Carmo RMD, Silva CMS, Silva GFF, Correa JPO, Notini MM, Freschi L, Cubas P, Nogueira FTS. 2023. Tomato miR156-targeted *SlSBP15* represses shoot branching by modulating hormone dynamics and interacting with *GOBLET* and *BRANCHED1b***.** *Journal of Experimental Botany* **74(17)**: 5124–5139.

Bhering LL. 2017. Rbio: A Tool For Biometric And Statistical Analysis Using The R Platform. *Crop Breeding and Applied Biotechnology* **17**: 187–190

Chen T, Zhou Y, Zhang J, Peng Y, Yang X, Hao Z, Lu Y, Wu W, Cheng T, Shi J, Chen J. 2021. Integrative analysis of transcriptome and proteome revealed nectary and nectar traits in the plant-pollinator interaction of *Nitraria tangutorum* Bobrov. *BMC Plant Biology* **21(1)**:230.

Bowman JL, Smyth DR.1999. *CRABS CLAW*, a gene that regulates carpel and nectary development in *Arabidopsis*, encodes a novel protein with zinc finger and helix-loop-helix domains. *Development* **126:** 2387–2396.

Cardoso-Gustavson P, Andreazza NL, Sawaya ACHF, Castro MM. **2013**. Only Attract Ants? The Versatility of Petiolar Extrafloral Nectaries in *Passiflora*. *American Journal of Plant Sciences* **4**: 460–469

Chandran D, Reinders A, Ward JM. 2003. Substrate specificity of the *Arabidopsis* thaliana sucrose transporter *AtSUC2*. *Journal of Biological Chemistry* **278(45)**: 44320–44325.

Chatt EC, Mahalim SN, Mohd-Fadzil NA, Roy R, Klinkenberg PM, Horner HT, Hampton M, Carter CJ, Nikolau BJ. 2021. Nectar biosynthesis is conserved among floral and extrafloral nectaries. *Plant Physiology* **185(4): 1595-1616**.

Cutri L, Dornelas MC. 2012. PASSIOMA: exploring expressed sequence tags during flower development in *Passiflora* spp. *International Journal of Genomics* **12**: 1–11.

Chitwood DH, Otoni WC. **2017a.** Morphometric analysis of *Passiflora* leaves: the relationship between landmarks of the vasculature and elliptical Fourier descriptors of the Blade. *GigaScience* **6(1)**: giw008

Chitwood DH, Otoni WC. **2017b**. Divergent leaf shapes among *Passiflora* species arise from a shared juvenile morphology. *Plant Direct* **1(5)**: e00028

Dai X, Zhuang Z, Zhao PX. 2018. psRNATarget: a plant small RNA target analysis server (2017 release). *Nucleic Acids Research* **46(W1)**: W49–W54.

Díaz-Riquelme J, Grimplet J, Martínez-Zapater JM, Carmona MJ. **2012**. Transcriptome variation along bud development in grapevine (*Vitis vinifera* L.). *BMC Plant Biology* **12**:181

Dolezel J., Greilhuber J. Lucretti S., Meister A., Lysak MA, Nardi L, Obermayer R. 1998. Plant genome size estimation by flow cytometry: inter-laboratory comparison. *Annals of Botany* **82**: 17–26.

Doležel J, Bartoš J. 2005. Plant DNA flow cytometry and estimation of nuclear genome size. *Annals of Botany* **95(1):** 99–110.

Doody E, Zha Y, He J, Poethig RS. 2022. The genetic basis of natural variation in the timing of vegetative phase change in *Arabidopsis thaliana*. *Development* **149(10)**: dev200321.

Elias TS. 1983. Extrafloral nectaries: their structure and distribution. *The biology of nectaries*. In: Bentley, B.L. and Elias, T.S., Eds. The Biology of Nectaries, Columbia University Press, New York, 174–203.

Eshed Y, Baum S F, Bowman J L. 1999. Distinct mechanisms promote polarity establishment in carpels of *Arabidopsis*. *Cell* **99(2)**: 199–209.

Ferigolo LS, Vicente MH, Correa JPO, Barrera-Rojas CH, Silva EM, Silva GFF, Carvalho Jr A, Peres LEP, Ambrosano GB, Margarido GRA, Sablowski R, Nogueira FTS. 2023. Gibberellin and the miRNA156-targeted SlSBPs synergistically regulate tomato floral meristem determinacy and ovary patterning. *Development* **150(21):** dev201961.

Feng S, Xu Y, Guo C, Zheng J, Zhou B, Zhang Y, Ding Y, Zhang L, Zhu Z, Wang H, Wu G. 2016. Modulation of miR156 to identify traits associated with vegetative phase change in tobacco (*Nicotiana tabacum*). *Journal of Experimental Botany* **67**: 1493–1504

Feuillet C, MacDougal M. 2007. Passifloraceae. In: Kubitzki K (Eds) Flowering Plants Eudicots. The families and genera of vascular plants. Springer, Berlin, Heidelberg **9**:270–281

Fouracre JP, He J, Chen V J, Sidoli S, Poethig RS. 2021. *VAL* genes regulate vegetative phase change via miR156-dependent and independent mechanisms. *PLoS Genetics* **17(6)**: e1009626.

Fu C, Sunkar R, Zhou C, Shen H, Zhang JY, Matts J, Wolf J, Mann DGJ, Stewart CN, Tang Y, Wang ZY. 2012. Overexpression of miR156 in switchgrass (*Panicum virgatum* L.) results in various morphological alterations and leads to improved biomass production. *Plant Biotechnology Journal* **10**:443–45

Gao R, Wang Y, Gruber MY, Hannoufa A. 2018. miR156/*SPL10* Modulates Lateral Root Development, Branching and Leaf Morphology in *Arabidopsis* by Silencing *AGAMOUS-LIKE 79*. *Frontiers in Plant Science* **8**:2226.

Guindon S, Dufayard JF, Lefort V, Anisimova M, Hordijk W, Gascuel O. 2010. New algorithms and methods to estimate maximum-likelihood phylogenies: assessing the performance of PhyML 3.0**.** *Systematic Biology* **59(3):** 307–321.

Gou J, Fu C, Liu S, Tang C, Debnath S, Flanagan, Flanagan A, Ge Y, Tang Y, Jiang Q, Larson PR, Wen J, Wang, Z. Y. 2017. The miR156-*SPL*4 module predominantly regulates aerial axillary bud formation and controls shoot architecture. *New Phytologist* **216(3)**: 829–840.

Guo Q, Li L, Zhao K, Yao W, Cheng Z, Zhou B, Jiang T. **2021**. Genome-wide analysis of poplar *Squamosa-Promoter-Binding Protein* (SBP) family under salt stress. *Forests* **12(4)**: 413.

He J, Xu M, Willmann MR, McCormick K, Hu T, Yang L, Starker CG, Voytas DF, Meyers BC, Poethig RS. 2018. Threshold-dependent repression of *SPL* gene expression by miR156/miR157 controls vegetative phase change in *Arabidopsis thaliana*. *PLoS Genetics* **14**: e1007337

Heil M. 2011. Nectar: generation, regulation and ecological functions. *Trends in Plant Science* **16(4)**: 191–200.

Heil M. 2015. Extrafloral nectar at the plant-insect interface: a spotlight on chemical ecology, phenotypic plasticity, and food webs. *Annual Review of Entomology* **60**: 213–232.

Hou H, Li J, Gao M, Singer SD, Wang H, Mao L, Fei Z, Wang X. **2013**. Genomic Organization, phylogenetic comparison and differential expression of the SBP-Box family genes in grape. *PLoS ONE* **8(3)**: e59358.

Hu T, Manuela D, Xu M. 2023. *SQUAMOSA PROMOTER BINDING PROTEIN-LIKE 9* and *13* repress *BLADE-ON-PETIOLE 1* and *2* directly to promote adult leaf morphology in *Arabidopsis*. *Journal of Experimental Botany* **74(6)**: 1926–1939.

Hu W, Qin W, Jin Y, Wang P, Yan Q, Li F, Yang Z. 2020. Genetic and evolution analysis of extrafloral nectary in cotton. *Plant Biotechnology journal* **18(10)**: 2081–2095.

Husbands AY, Benkovics AH, Nogueira FTS, Lodha M, Timmermans MC. 2015. The ASYMMETRIC LEAVES Complex Employs Multiple Modes of Regulation to Affect Adaxial-Abaxial Patterning and Leaf Complexity. *Plant Cell* **27(12)**:3321–35.

Izaguirre MM, Mazza CA, Astigueta MS, Ciarla AM, Ballaré CL. 2013. No time for candy: Passionfruit (*Passiflora edulis*) plants down-regulate damage-induced extra floral nectar production in response to light signals of competition. *Oecologia* **173**: 213–221.

Johnson C R, Millwood R J, Tang Y, Gou J, Sykes R W, Turner G B, Davis MF, Sang Y, Wang ZY, Stewart CN. 2017. Field-grown miR156 transgenic switchgrass reproduction, yield, global gene expression analysis, and bioconfinement. *Biotechnology for Biofuels* 10: 1–12.

Karnovsky JM. 1965. A formaldehyde glutaraldehyde fixative of high osmolality for use in electron microscopy. *Journal of Cell Biology* **27**: 137.

Kasprzewska A, Carter R, Swarup R, Bennett M, Monk N, Hobbs JK, Fleming A. 2015. Auxin influx importers modulate serration along the leaf margin. *The Plant Journal* **83(4)**:705–18.

Killip EP. 1938. The American species of Passifloraceae. *The American species of Passifloraceae.*, 407:407–408

Kram B W, Xu WW, Carter CJ. 2009. Uncovering the *Arabidopsis thaliana* nectary transcriptome: investigation of differential gene expression in floral nectariferous tissues. *BMC Plant Biology* **9:**92.

Krosnick S, Gasser C, Potter D. **2011**. *Passiflora* as a model system for studying nectary diversification: insights and implications. Abstract book of the XVI International Botanical Conference (IBC2011, Melbourne, Australia): 63–64.

Kwok KE, Laird RA. 2012. Plant age and the inducibility of extrafloral nectaries in *Vicia faba*. *Plant Ecology* **213**: 1823–1832

Lawrence EH, Leichty AR, Doody EE, Ma C, Strauss SH, Poethig RS. 2021. Vegetative phase change in *Populus tremula* x *alba*. *New Phytologist* **231**:351−64

Lee JY, Baum SF, Oh SH, Jiang CZ, Chen JC, Bowman JL. **2005**. Recruitment of *CRABS CLAW* to promote nectary development within the eudicot clade. *Development* **132**: 5021–5032

Lefort V, Longueville JE, Gascuel O. 2017. SMS: Smart Model Selection in PhyML. *Molecular Biology and Evolution* **34(9)**: 2422-2424.

Leichty AR, Poethig RS. 2019. Development and evolution of age-dependent defenses in ant-acacias. *Proceedings of the National Academy of Sciences, USA*, **116**: 15596–15601.

Lemos RCC, Costa Silva D, Albuquerque Melo-de-Pinna GF. **2017**. A structural review of foliar glands in *Passiflora* L. (Passifloraceae). *PLoS ONE* **12(11):** e0187905.

Letunic I, Bork P. **2021**. Interactive tree of life (iTOL) v5: An online tool for phylogenetic tree di*SPL*ay and annotation. *Nucleic Acids Research* **49**: W293–W296

Li XM, Jenke H, Strauss S, Bazakos C, Mosca G, Lymbouridou R, Kierzkowski D, Neumann U, Naik P, Huijser P, Laurent S, Smith RS, Runions A, Tsiantis M. 2024. Cell-cycle-linked growth reprogramming encodes developmental time into leaf morphogenesis. *Current Biology* **34(3)**:541–556

Livak KJ, Schmittgen TD. **2001**. Analysis of relative gene expression data using real-time quantitative PCR and the $2^{-\Delta\Delta CT}$ method. *Methods* **25**: 402–408

Loureiro J, Rodriguez E, Doležel J, Santos C. 2007. Two new nuclear isolation buffers for plant DNA flow cytometry: A test with 37 species. *Annals of Botany*, **100**: 875–888.

Macêdo LPM, Silva EO, Aguiar-Dias ACA. **2021**. Morphoanatomy and ecology of the extrafloral nectaries in two species of *Passiflora* L. (Passifloraceae). *South African Journal of Botany* **143**: 248–255.

Machado KLG, Faria DV, Duarte MBS, Silva LAS, Oliveira TR, Falcão TCA, Batista DS, Costa MGC, Santa-Catarina C, Silveira V, Romanel E, Otoni WC, Nogueira FTS. 2023. Plant age-dependent dynamics of annatto pigment (bixin) biosynthesis in *Bixa orellana* L. *Journal of Experimental Botany* **17**:erad458.

Madeira F, Pearce M, Tivey ARN, Basutkar P, Lee J, Edbali O, Madhusoodanan N, Kolesnikov A, Lopez R. **2022**. Search and sequence analysis tools services from EMBL-EBI. *Nucleic Acids Research* **50**: W276–W279

Manders G, Otoni WC, d'Utra Vaz F B, Blackball NW, Power JB, Davey MR. **1994.** Transformation of passionfruit (*Passiflora edulis* fv flavicarpa Degener.) using *Agrobacterium tumefaciens*. *Plant Cell Reports* **13**: 697–702.

Manni M, Berkeley MR, Seppey M, Simão FA, Zdobnov, E M. **2021.** BUSCO update: novel and streamlined workflows along with broader and deeper phylogenetic coverage for scoring of eukaryotic, prokaryotic, and viral genomes. *Molecular Biology and Evolution* **38(10):** 4647–4654.

Marazzi B, Bronstein JL, Koptur S. 2013. The diversity, ecology and evolution of extrafloral nectaries: current perspectives and future challenges. *Annals of Botany* **111(6)**: 1243–1250.

Moraes TS, Rossi ML, Martinelli AP, Dornelas MC. 2022. Morphological and anatomical traits during development: Highlighting extrafloral nectaries in *Passiflora organensis*. *Microscopy Research Technique* **85**: 2784–2794

Morris S E, Turnbull C G, Murfet IC, Beveridge CA. 2001. Mutational analysis of branching in pea. Evidence that Rms1 and Rms5 regulate the same novel signal. *Plant Physiology* **126(3):**1205–1213.

Murashige T, Skoog F. **1962**. A Revised Medium for Rapid Growth and Bio Assays with Tobacco Tissue Cultures. *Physiologia Plantarum* **15**: 473–497

Nakayama H, Leichty A R, Sinha N R. 2022. Molecular mechanisms underlying leaf development, morphological diversification, and beyond. *The Plant Cell* **34(7)**: 2534–2548

O'Brien, TP, McCully, ME. 1981. The study of plant structure: principles and selected methods. Termarcarphi PTY, Melbourne.

Ostria-Gallardo E, Ranjan A, Chitwood DH, Kumar R, Townsley BT, Ichihashi Y, Corcuera LJ, Sinha NR. 2016. Transcriptomic analysis suggests a key role for *SQUAMOSA PROMOTER BINDING PROTEIN LIKE*, *NAC* and *YUCCA* genes in the heteroblastic development of the temperate rainforest tree *Gevuina avellana* (Proteaceae). *New Phytologist* **210(2)**: 694–708

Ortiz-Sepulveda CM, Van Bocxlaer B, Meneses AD, Fernández F. 2019. Molecular and morphological recognition of species boundaries in the neglected ant genus *Brachymyrmex* (Hymenoptera: Formicidae): toward a taxonomic revision. *Organisms Diversity & Evolution* **19:** 447–542.

Otoni WC, Silva ML, Lima ABP, Paim Pinto DL, Lani ERG, Reis LB. 2007. Transformação genética de maracujazeiros. In: Torres, AC, Dusi, AN and Santos, MDM (eds) Transformação Genética de Plantas via *Agrobacterium*: Teoria e Prática. EMBRAPA Hortaliças, Brasília, DF. pp. 125–141

Pei Y, Zhang J, Wu P, Ye L, Yang D, Chen J, Li J, Hu Y, Zhu X. **2021** GoNe encoding a class VIIIb *AP2 / ERF* is required for both extrafloral and floral nectary development in Gossypium. *The Plant Journal* **106**:1116–1127

Pérez JO, d'Eeckenbrugge GC. 2017. Morphological characterization in the genus *Passiflora* L.: an approach to understanding its complex variability. *Plant Systematics and Evolution* **303**: 531–558

Poethig RS. **2013**. Vegetative phase change and shoot maturation in plants. *Current Topics in Developmental Biology* **115**:125–152

Poethig RS, Fouracre J. 2024. Temporal regulation of vegetative phase change in plants. *Developmental Cell* **59(**1): 4–19

Preston JC, Hileman LC. **2013**. Functional evolution in the plant *SQUAMOSA-PROMOTER BINDING PROTEIN-LIKE* (*SPL*) gene family. *Frontiers in Plant Science* **4**: 80

Rocha DI, Silva LC, Valente VMM, Francino DMT, Meira RMSA. **2009**. Morphoanatomy and development of leaf secretory structures in *Passiflora amethystina* Mikan (Passifloraceae). *Australian Journal of Botany* **57(7)**: 619–626

Salazar GA, Sonnhammer ELL, Tosatto SCE, Paladin L, Raj S, Richardson LJ, Finn RD, Bateman A. 2020. Pfam: The protein families database in 2021. *Nucleic Acids Research* **49(D1)**: D412–D419.

Salinas M, Xing S, Höhmann S, Berndtgen R, Huijser P. **2012**. Genomic organization, phylogenetic comparison and differential expression of the SBP-box family of transcription factors in tomato. *Planta* **235**: 1171–1184

Siegfried KR, Eshed Y, Baum SF, Otsuga D, Drews GN, Bowman, JL. 1999. Members of the YABBY gene family specify abaxial cell fate in *Arabidopsis*. *Development* **126:** 4117–4128

Silva GFFE, Silva EM, Da Silva Azevedo M, Guivin MAC, Ramiro DA, Figueiredo CR, Carrer H, Peres LEP, Nogueira FTS. **2014**. MicroRNA156-targeted *SPL/SBP* box transcription factors regulate tomato ovary and fruit development. *The Plant Journal* **78**: 604–618

Silva PO, Batista DS, Cavalcanti JHF, Koehler AD, Vieira LM, Fernandes AM, Barrera-Rojas CH, Ribeiro DM, Nogueira FTS, Otoni WC. **2019**. Leaf heteroblasty in *Passiflora edulis* as revealed by metabolic profiling and expression analyses of the microRNAs miR156 and miR172. *Annals of Botany* **123**: 1191–1203

Silveira M. 1989. Preparo de amostras biológicas para microscopia eletrônica de varredura. In: Souza W. (editor). Manual sobre técnicas básicas em microscopia eletrônica. v.1. Sociedade Brasileira de Microscopia Eletrônica, Rio de Janeiro. pp. 71–79

Schneider CA, Rasband WS,Eliceiri KW. 2012. NIH Image to ImageJ: 25 years of image analysis. *Nature Methods* **9**: 671–675

Slavković F, Dogimont C, Morin H, Boualem A, Bendahmane A. 2021. The genetic control of nectary development. *Trends in Plant Science* **26(3)**: 260–271.

Tang HB, Wang J, Wang L, Shang GD, Xu ZG, Mai YX, Liu YT, Zhang TQ, Wang JW. 2023. Anisotropic cell growth at the leaf base promotes age-related changes in leaf shape in *Arabidopsis thaliana*. *The Plant Cell* **35 (5)**:1386–1407.

Ulmer T, MacDougal J M. 2004. *Passiflora*: Passionflowers of the world. Timber Press.

Varkonyi-Gasic E, Wu R, Wood M, Walton EF, Hellens RP. **2007.** Protocol: A highly sensitive RT-PCR method for detection and quantification of microRNAs. *Plant Methods* **3:**12

Villamil N, Márquez-Guzmán J, Boege K. 2013. Understanding ontogenetic trajectories of indirect defence: ecological and anatomical constraints in the production of extrafloral nectaries. *Annals of Botany* **112 (4)**: 701–709.

Xu M, Hu T, Zhao J, Park M-Y, Earley KW, Wu G, Yang L, Poethig RS. **2016**. Developmental Functions of miR156-Regulated *SQUAMOSA PROMOTER BINDING PROTEIN-LIKE* (*SPL*) Genes in *Arabidopsis thaliana*. *PLOS Genetics* **12**: e1006263

Wang JW, Czech B, Weigel D. 2009. miR156-regulated *SPL* Transcription Factors define an endogenous flowering pathway in *Arabidopsis thaliana*. *Cell* **138**: 738–749

Wu G, Park MY, Conway SR, Wang JW, Weigel D, Poethig RS. 2009. The sequential action of miR156 and miR172 regulates developmental timing in *Arabidopsis*. *Cell* **138**: 750–759

Wu Z, Cao Y, Yang R, Qi T, Hang Y, Lin H, Zhou G, Wang ZY, Fu C. 2016. Switchgrass SBP-box transcription factors Pv*SPL*1 and 2 function redundantly to initiate side tillers and affect biomass yield of energy crop. *Biotechnology for Biofuels* **9**: 1–15.

Yang L, Xu M, Koo Y, He J, Poethig RS. 2013. Sugar promotes vegetative phase change in *Arabidopsis thaliana* by repressing the expression of *MIR156A* and *MIR156C*. *elife* **2:** e00260.

Yu N, Cai WJ, Wang S, Shan CM, Wang LJ, Chena XY. **2010**. Temporal control of trichome distribution by microRNA156-targeted *SPL* genes in *Arabidopsis thaliana*. *The Plant Cell* **22**: 2322–2335

Zhao J, Doody E, Poethig RS. 2023. Reproductive competence is regulated independently of vegetative phase change in *Arabidopsis thaliana*. *Current Biology* **33(3)**: 487–497.

7. Supplementary Material

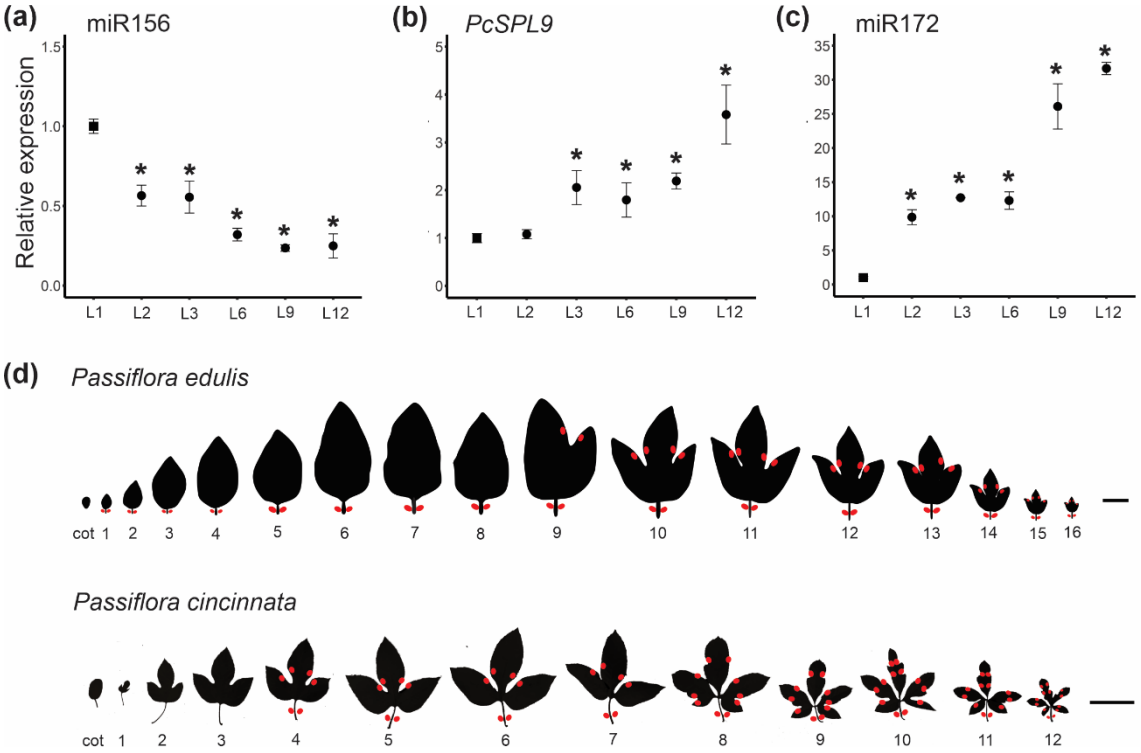

Supplementary Figure 1: Expression patterns of microRNAs and *SPL9* during the heteroblastic leaf development. (a-c) Expression patterns of miR156 **(a)**, *PcSPL9* **(b)**, and miR172 **(c)** in *Passiflora cincinnata* leaf primordia. Values are mean ± SE (n=3-4). *$P \leq 0.05$ (Student's *t*-test). **(d)** Overview of leaf heteroblastic development and location of extrafloral nectary (in red) in *Passiflora* species. Left to right, from young to adult leaves. Cot, cotyledons. Scale Bar: 2 cm; 10 cm.

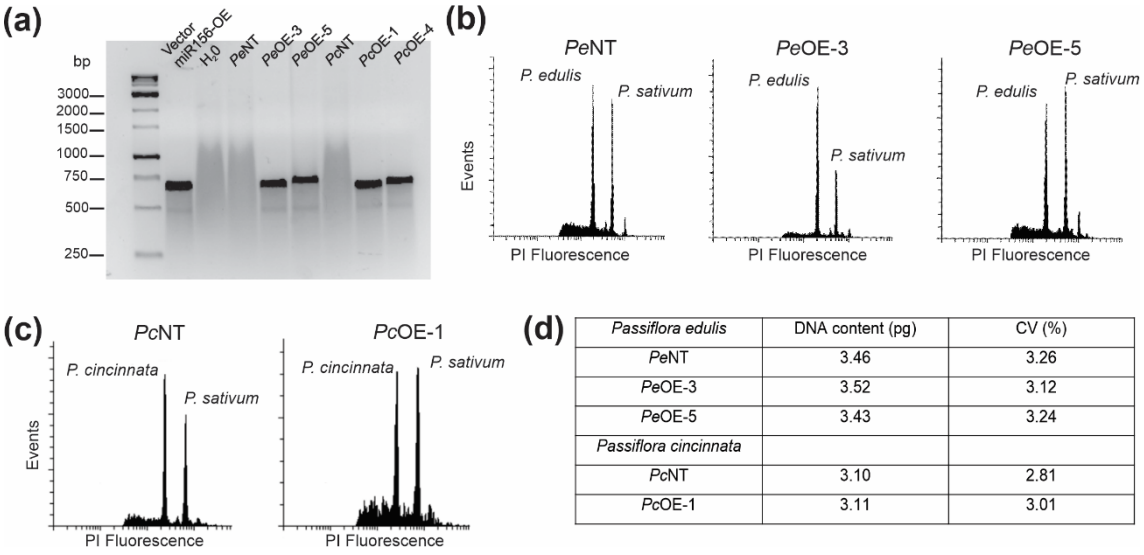

Passiflora edulis	DNA content (pg)	CV (%)
*Pe*NT	3.46	3.26
*Pe*OE-3	3.52	3.12
*Pe*OE-5	3.43	3.24
Passiflora cincinnata		
*Pc*NT	3.10	2.81
*Pc*OE-1	3.11	3.01

Supplementary Figure 2: Transgenic molecular characterization and estimation of nuclear DNA content. (a) PCR amplification confirming the presence of the *hpt*II gene for hygromycin resistance in miR156-overexpressing plants (amplicon = 558 bp). **(b, c)** Flow cytometry analysis of non-transformed (*Pe*NT) and miR156-overexpressing events in *Passiflora edulis* (*Pe*OE-3 and *Pe*OE-5) **(b)**, and *Passiflora cincinnata* non-transformed (*Pc*NT) and miR156-overexpressing event (*Pc*OE-1) **(c)**. Each histogram first and second peaks correspond to the *Passiflora* and the *Pisum sativum* internal standard (2C = 9.09 pg of nuclear DNA). **(d)** Means of DNA content, determined by flow cytometry, in NT and miR156-overexpressing events. CV (%): Coefficient of variation.

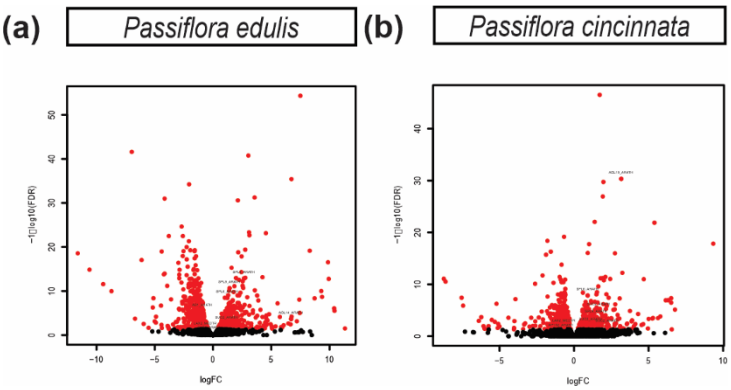

Supplementary Figure 3: Distribution of differentially expressed genes (DEGs) from the RNA-seq data. (a) Volcano plot of DEGs representing up- (LogFC >0) and down-regulated (LogFC<0) genes in red color from non-transgenic vs miR156-overexpressing **(a)** *Passiflora edulis* and (**b**) *P. cincinnata* leaf primordia.

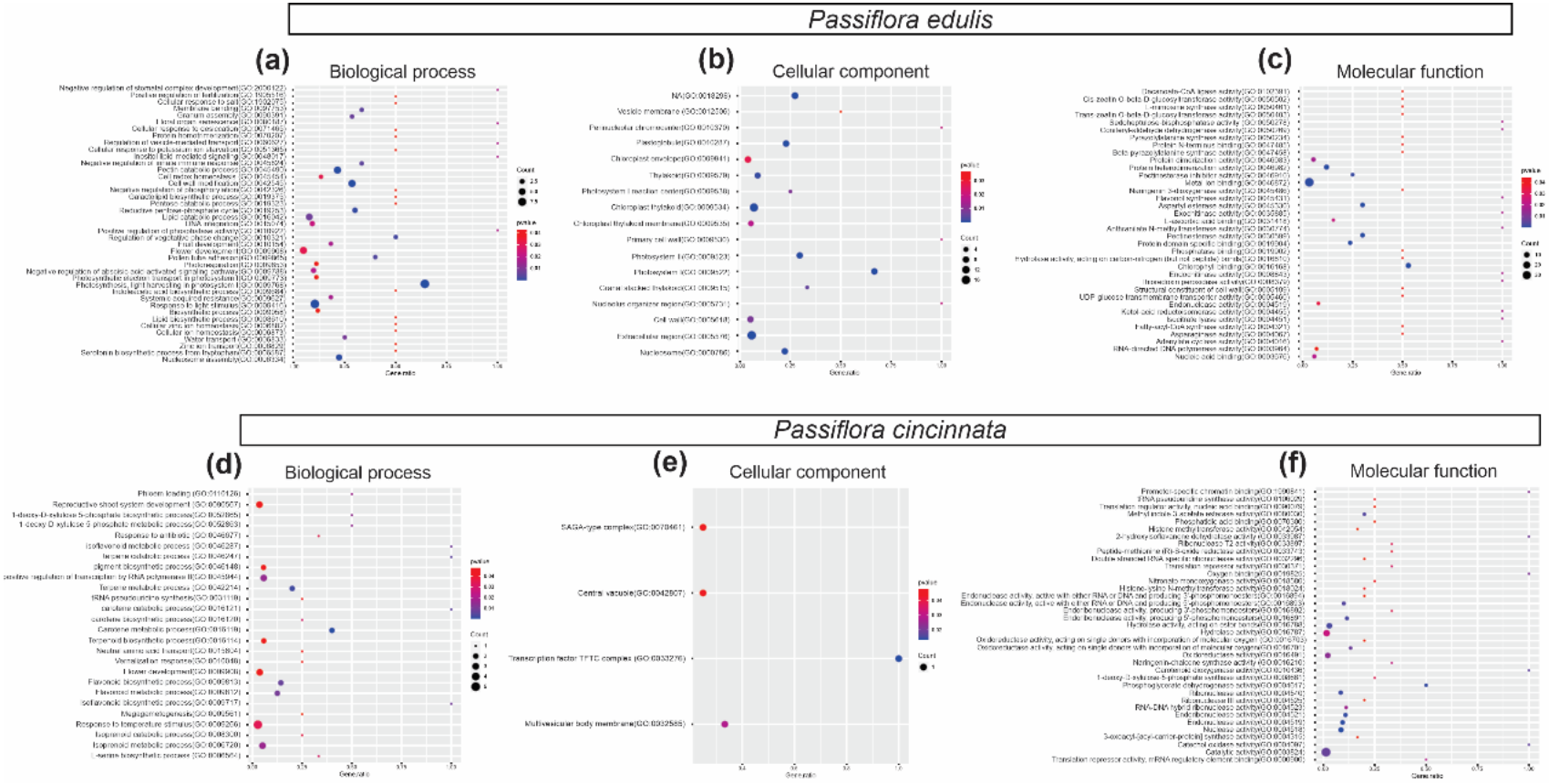

Supplementary Figure 4 –. Gene Ontology enrichment of DEGs in miR156-overexpressing versus non-transgenic plants. **(a)** Biological process **(b)** cellular component and **(c)** Molecular function in *Passiflora edulis*. **(d)** Biological process **(e)** cellular component and **(f)** Molecular function in *Passiflora cincinnata*. The dot size represents the number of DEGs associated with the process (count) and the dot color represents the significance of the enrichment (p-value ≤ 0.05).

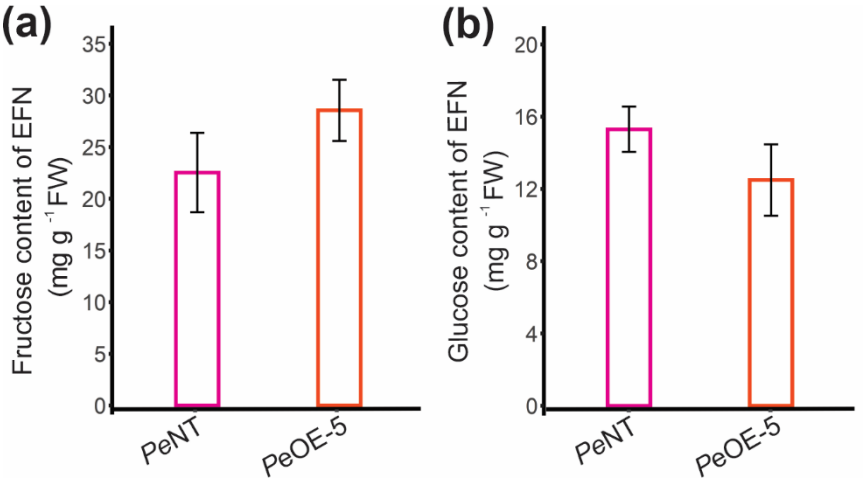

Supplementary Figure 5: (a) Fructose and **(b)** glucose content of the laminar and petiolar extrafloral nectary pool of *Passiflora edulis* non-transgenic (*Pe*NT) and miR156 overexpressor (*Pc*OE-5) (n= 3).

Supplementary Table S1. Oligonucleotide sequences used in this study.

Table S1. Oligonucleotide sequences used in molecular characterization.		
Name	**Sequence**	**Purpose**
HPTII F	GAATTCAGCGAGAGCCTGAC	RT-PCR
HPTII R	ATTTCGGCTCCAACAATGT	RT-PCR
miR156 F	GCGGCGTTGACAGAAGAGAGT	RT-qPCR
miR156/7 _ RT R	GTTGGCTCTGGTGCAGGGTCCGAGGT ATTCGCACCAGAGCCAACGTGCTC	cDNA synthesis
Reverse universal	GTGCAGGGTCCGAGGT	RT-qPCR
PeACT F	CCAGGCATTGCTGATAGGAT	RT-qPCR
PeACT R	ATTCTGCCTTTGCAATCCAC	RT-qPCR
*SPL*4 F	GTTCTGTCGAGTCCTATGC	RT-qPCR
*SPL*4 R	TCCCTGGAAGTGTCATCT	RT-qPCR
*SPL*6 F	TTACCACAAGAGGCACAAAG	RT-qPCR
*SPL*6 R	CCTGCTACACTGTTGACAAA	RT-qPCR
Pc*SPL*9 F	AGGTGGAAGGATGCAAAG	RT-qPCR
Pc*SPL*9 R	GCTCTAAACCAGCAACAATG	RT-qPCR
Pe*SPL*9 F	GGTCTAACCCAAATCCCGCA	RT-qPCR
Pe*SPL*9 R	AGAGACCAGTGTGTGTGATGAG	RT-qPCR
*SPL*13a F	CAATGTGCCTTGTCGATGG	RT-qPCR
*SPL*13a R	AGTAACCTGTGGAGTCTTGG	RT-qPCR
AS1 F	AGTCAGAGAAGTCATGCCGC	RT-qPCR
AS1 R	TCTGCTCCTTGGCTTCTGC	RT-qPCR
YAB1F	GTTTCATTTGGGACATGGTTTCT	RT-qPCR
YAB1 R	CTCGTTTGGATTTGGCTGATTG	RT-qPCR
YAB5 F	AAAGGCAGCGAGTACCTTC	RT-qPCR
YAB5 R	TGCTTCTCTGTGGCTGAT	RT-qPCR
SUC-like F	ATACGTGCAACTCCTTGGCA	RT-qPCR
SUC-like R	GGAGGTGCAACGGTCACTAT	RT-qPCR
LAX2 F	GATCAACTCCTCGACCATTC	RT-qPCR
LAX2 R	GGTACATGCAAACCCGAA	RT-qPCR

PeAGL104 F	CGCAAGGCTACAGCAACAATTTC	RT-qPCR
PeAGL104 R	TTCTCACATGATTCAAGCTCC	RT-qPCR
Pe*SPL*6 GSP R	CTCGCTGAAGCTGCGATGAC	5' RACE
Pe*SPL*6 NESTED GSP R	GACTCCCCTCTGCAGAACAC	5' RACE
Pe*SPL*13a GSP R	GGTGAGTTCCACTTGCAGATGACC	5' RACE
Pe*SPL*13a NESTED GSP R	GCCAAAACATCGGAACCACC	5' RACE

Supplementary Table S2. Differentially Expressed Genes (DEGs) in leaf primordia of non- transgenic vs miR156-overexpressing *Passiflora edulis*.

https://docs.google.com/spreadsheets/d/1XIhWn1N3_DbECn4Uv99r8WZncv8bvTKT/edit?usp=sharing&ouid=108718609711684561379&rtpof=true&sd=true

Supplementary Table S3. Differentially Expressed Genes (DEGs) in leaf primordia of non- transgenic vs miR156-overexpressing *Passiflora cincinnata***.**

https://docs.google.com/spreadsheets/d/1X1duUHswsa6inRdrn_JsLL6WhQFTpHmD/edit?usp=sharing&ouid=108718609711684561379&rtpof=true&sd=true

Supplementary Table S4. Characteristics of *SPL/SBPs* genes in *Passiflora* species and the miR156 recognition region.

https://docs.google.com/spreadsheets/d/1aNp_zOaJBhoWSMPX_RngtLoBhRXruCqg/edit?usp=sharing&ouid=108718609711684561379&rtpof=true&sd=true

Supplementary Table S5. Putative miR156 targets in *Passiflora edulis* identified using the psRNATarget tool.

https://docs.google.com/spreadsheets/d/1_MppdZSDsRc_wNLtVsvBTemIl5PxvPxJ/edit?usp=sharing&ouid=108718609711684561379&rtpof=true&sd=true